The transcription factor CLAMP is required for neurogenesis in *Drosophila melanogaster*.

Maria A. Tsiarli [1,2,*], Ashley M. Conard [1,3,4], Lucy Xu [1], Erica Nguyen[1], Erica N. Larschan [1,*]

[1] Department of Molecular Biology, Cellular Biology and Biochemistry, Brown University, Providence, RI 02912, USA

[2] Department of Neurobiology, Harvard Medical School, Boston, MA Department 02115, USA

[3] Center for Computational and Molecular Biology, Brown University, Providence, RI, 02912;

[4] Computer Science Department, Brown University, Providence, RI, 02912

* corresponding author

Contact information

Maria A. Tsiarli: maria_tsiarli@brown.edu; maria_tsiarli@hms.harvard.edu

Ashley M. Conard: ashley_conard@brown.edu

Lucy Xu: lucy_xu@alumni.brown.edu

Erica Nguyen: erica_nguyen@alumni.brown.edu

Erica N. Larschan: erica_larschan@brown.edu

Abstract

Neural stem cell (NSC) differentiation is controlled by cell-intrinsic and external signals from the stem cell niche including niche surface glia (SG). However, the mechanisms by which transcription factors drive NSC differentiation within the niche remain largely unknown. Here, we show that the transcription factor, Chromatin-linked adaptor for MSL proteins (CLAMP) is required for NSC differentiation. CLAMP promotes transcription of genes involved in stemness, proliferation, and glial development and represses transcription of genes involved in neurogenesis and niche survival. Consistent with transcriptional changes, CLAMP promotes NSC proliferation and SG production. Furthermore, glial-specific knock-down of *clamp* causes similar phenotypes to *clamp* null mutants. CLAMP motifs are present at many target genes including the glial-determining gene, *glial cells missing,* and *Notch,* a key regulator of neurogenesis. Collectively, our results suggest that CLAMP regulates a transcriptional program which drives NSC proliferation and differentiation *via* cell-intrinsic and niche-dependent mechanisms that involve niche glia.

52 **Introduction**

53

54 Brain development is an extremely complex yet carefully orchestrated process, regulated along
55 spatiotemporal axes. For the formation of the functional brain circuitry to take place, neural stem cells
56 (NSCs) must undergo multiple rounds of divisions and lineage decisions at each step of the process are
57 governed by specific transcription factors (TFs)[1]. In addition to the intrinsic developmental program,
58 external metabolic and paracrine signals constitute another layer of developmental control over NSCs.
59 Specifically, NSCs are part of a specialized microenvironment, the stem cell niche[2], which plays an
60 architectural and nurturing role for the NSCs and their progeny. Moreover, the niche serves as a hub for the
61 relay of metabolic and developmental signals that regulate differentiation of NSCs in order for the proper
62 sequence of developmental events to be maintained[3]. In mammals, the stem cell niche is composed of
63 various cell populations including neurons, glial cells, resident immune cells, the microglia, blood vessels
64 which along with endothelial cells and glial cells form the blood-brain-barrier[4]. In *Drosophila*, the stem cell
65 niche also consists of the NSCs, NSC progeny and glial cells of various types that are vital to the
66 maintenance of the homeostatic balance required for proper neurogenesis to take place[3,5-10]. However, little
67 is understood about the gene regulatory mechanisms that generate the stem cell niche.

68

69 In *Drosophila melanogaster* neurogenesis occurs at two distinct stages: the embryonic and post-embryonic
70 stages [11,12]. The *Drosophila* central nervous system (CNS) is composed of the central brain (CB), the optic
71 lobe (OL) and the ventral nerve cord (VNC). During the embryonic stage, CB neural stem cells (neuroblasts
72 in *Drosophila*) proliferate to generate primary neurons until they become quiescent at the end of the
73 embryonic stage. The optic lobe primordium which would form the OL, is generated by epithelial cells of
74 the posterior procephalic region between embryonic stages 11-13[13]. Between stages 12-13 the OL
75 primordium invaginates and attaches at the ventrolateral surface of the brain and embryonic OL neuroblasts
76 (EONs) are formed[14]. EONs proliferate briefly to generate both glial and neuronal progeny and also enter

77 quiescence [14,15]. Then during the early larval stage, concurrent with the initiation of larval feeding, metabolic
78 signals impinge on the NSCs and cause exit from quiescence and initiation of the neurogenesis.
79
80 Neural stem cells divide asymmetrically, such that in each division they generate a new NSC and a daughter
81 cell which will generate glial and/or neuronal progeny[16]. For the appropriate asymmetric division to take
82 place, polarity determinants have to be sequestered on the apical and basal sides of the mother NSC: the
83 apical complexes are inherited by the new NSC and maintain the proliferating state, whereas basal proteins
84 are inherited by the daughter cell and will direct it to generate differentiated lineages. The Par protein
85 complex which is apically localized also directs the localization of the basal determinants. Moreover, Par
86 complex proteins such as the *Inscuteable* (Insc) and *Partner of Inscuteable (Pins)* regulate the orientation
87 of the mitotic spindle which determines how the cleavage furrow will form during the division of the NSC
88 [17,18].
89
90 In the *Drosophila* five distinct CNS glial types are identified based on morphological, positioning and
91 molecular profile criteria: perineurial (PG), subperineurial glia (SPG), cortex glia (CG), astrocyte-like and
92 ensheathing glia[19]. The first two types of glia constitute the *Drosophila* brain-blood barrier whereas PG,
93 SPG and CG can also be classified as surface glia because they are closer to the brain surface[15]. Perineural
94 glia are found on the outside layer of the CNS and serve a nurturing role for the development and function
95 of the NSCs and also regulate NSC proliferation *via* the secretion of Dally-like heparan sulfate proteoglycan
96 (Dlp)[5]. Reciprocally, the proliferating NSCs secrete the BMP homologue, Glass bottom boat (Gbb) which
97 acts to regulate their proliferation but also provides a survival signal to PG. This study also suggests that
98 PG and NSCs have direct communication *via* direct membrane contact or transcytosis. SPG glia forms a
99 tight protective layer of pleated septate junction contacts thus providing insulation of the nervous system
100 from exogenous molecules. With the initiation of larval feeding, SPG and PG contribute to the reactivation
101 of quiescent NSCs [5,8,20] *via* fat body signaling and induction of insulin secretion from SPG. In conditions
102 of oxidative stress and hypoxia, SPG and CG form lipid droplets (LDs) which protect NSCs from oxidative

103 stress [6,21]. Cortex glia are especially interesting because these cells form a bespoke membrane chamber
104 around diving NSCs and their progeny, thus providing not only protection and bidirectional signaling
105 between the proliferating NSCs and their niche, but also serving as individual spatial units for each
106 expanding NSC and its progeny[3]. A special subtype of CG, *mir8*$^{+}$ surface-associated CG, controls
107 neurogenesis in the OL[13,19,22]. Thus, niche glia are important for the function of NSCs. However, the
108 molecular mechanisms that direct the functional and nurturing relationship between niche glia and NSCs
109 remain poorly understood.
110
111 Here we define a role for the essential CLAMP zinc finger TF[23] in neurogenesis which is partly mediated
112 by niche glia. *Clamp* was discovered as part of a screen for factors that are necessary for the function of the
113 dosage compensation machinery in *Drosophila melanogaster* males [24]. In contrast to the MSL complex
114 components, CLAMP is essential for viability of both males and females and has transcriptional targets on
115 all chromosomes, albeit with a stronger binding affinity on the X [23,25]. Since its first characterization as a
116 required link for the MSL complex to bind to the X-chromosome [26,27], CLAMP is emerging as a
117 multifaceted transcription factor with roles including chromatin organization [28], histone locus function [29]
118 and regulation of Pol II function [30]. The identification of *Clamp* (CG1832), as a functional interactor of
119 *embryonic lethal abnormal visual system* (*elav*) and *erect wings* (*ewg),* critical regulators of embryonic and
120 post-embryonic neural development, hinted at a neuronal role of CLAMP [31,32]. Therefore, we hypothesized
121 that CLAMP is a TF which regulates neuronal development and NSC biology.
122
123 To test our hypothesis, we investigated the role of CLAMP in nervous system development. We find that
124 CLAMP is important both for neuronal and glial cell generation and regulates NSC proliferation *via* cell-
125 intrinsic and niche-dependent mechanisms. We used a CRISPR/Cas9-generated frameshift mutant in the
126 *clamp* gene which eliminates the expression of the CLAMP protein [25] to determine that lack of CLAMP
127 results in defects in brain development. Specifically, *clamp* null mutants have a smaller brain than controls,
128 with the most prominent defect observed in the optic lobe which is almost entirely lost. Our mRNA-

129 sequencing data from *clamp* mutant embryos and larval brains followed by temporal gene ontology (GO)
130 analysis determined that CLAMP positively regulates stemness/NSC proliferation genes and glial-
131 development genes. Binding motif analysis revealed the CLAMP motifs are present at key neurogenesis
132 genes such as *bazooka, gbb* and the glial-development regulator, *glial cells missing.* We validated
133 transcriptomics by using immunostaining to show that *clamp* null mutants exhibit a brain-wide reduction
134 in proliferating NSCs and surface glia and a profound defect in the development of the OL. Knock-down
135 of *clamp* in glia but not in neurons, revealed that NSC proliferation and glia generation are regulated in part
136 *via* glial *clamp*. Our results support a model in which CLAMP promotes the precise timing of NSC
137 differentiation by regulating genes which drive intrinsic and niche-glial mechanisms.
138
139
140 **Results**
141
142 ***CLAMP is ubiquitously expressed throughout the L3 nervous system and is present in proliferating***
143 ***neuroblasts.***
144
145 *Clamp* is maternally deposited and therefore *clamp* transcript and protein levels [29] are present at high levels
146 during embryogenesis. Near the end of embryogenesis (16-18 hours) during tissue differentiation and the
147 cessation of the first wave of neurogenesis, *clamp* transcript levels show a reduction followed by a sharp
148 increase between 20-24 hours and then a decrease throughout the post-embryonic neurogenesis period (Fig.
149 1a). Tissue-specific expression data from modENCODE Development RNA-Seq Collection[33,34]/Flybase[35]
150 show that *clamp* is highly expressed in the L3 central nervous system (Fig.1a). To define the role of CLAMP
151 in neural development, we mapped its expression in the developing L3 nervous system.
152 Immunofluorescence for CLAMP in L3 larvae revealed that it is ubiquitously expressed in the nucleus
153 throughout the larval nervous system, both in cells of the brain and the ventral nerve cord (VNC), (Figs.1c-
154 g and h). Interestingly, a subset of processes in the VNC also show protein localization of CLAMP,

155 suggesting that it may be transported to neuronal arborizations (Fig. 1c, axonal processes indicated by
156 arrows). Co-staining with the neural stem cell (NSC) marker Deadpan (Dpn), revealed that CLAMP is
157 expressed in NSCs (Figs.1i, j). Interestingly, CLAMP maintains its expression in mitotic/proliferating
158 NSCs, as seen by co-staining of Dpn and PCNA, both in the central brain and the OL (Figs.1i, j). The
159 distribution of the TF PCNA[36] within the cell nucleus changes during the progression of the cell cycle
160 allowing its nuclear localization to mark distinct phases of the cell-cycle [37,38]. In this way, we determined
161 that CLAMP is present in S, G1 and G2-phase cells (Fig.1j).
162
163 ***Lack of CLAMP leads to deficits in larval development***
164
165 To determine the role of CLAMP in nervous system development, we characterized brain development in
166 *clamp*^{2} mutants which we previously generated in our lab *via* the CRISPR/Cas9 approach[25]. Specifically,
167 in these mutants, a frameshift mutation in the *clamp* gene abolishes expression of CLAMP protein[25] (from
168 here on referred as *clamp* null). Due to the requirement for CLAMP for the recruitment of the dosage
169 compensation complex in males [23], the majority of male larvae die at the L2 stage. In contrast, female larvae
170 die at the late L3/prepupa stage [25]. Because we are interested in the essential role of CLAMP outside of
171 dosage compensation and due to the small number of male *clamp* null larvae, we only used female larvae
172 and focused on the L3 stage when larval brains can be dissected. Additionally, we matched control animals
173 for developmental stage with the *clamp* null larvae (see Materials and methods for details). Comparison of
174 *clamp* null L3 larvae to controls revealed that they are significantly smaller in size than matched controls
175 (Figs.2a and b). Furthermore, macroscopic examination of the central nervous system of *clamp* null larvae
176 revealed that their brains are significantly smaller compared to controls (Figs.2c and d). Western blotting
177 for CLAMP in *clamp* null larvae brains verified the absence of CLAMP protein (Fig.2e).
178
179 ***Lack of CLAMP causes defects in brain development***
180

181 In order to evaluate CNS development in the clamp *null* mutants, for the majority of our experiments we
182 focused on the L3 stage and specifically the mid/late L3 stage (~120 hours after larval hatching (ALH)),
183 because the *clamp* mutants die during late L3/early pupa stage. Additionally, to better understand the extent
184 of neurodevelopmental defects in the *clamp* null animals, we also examined early L3 larvae brains. The
185 overall morphology of the CNS, as observed with DAPI staining, is different between nulls and controls as
186 described below (Figs.3a and e). As neural development progresses through the larval stages, the
187 neuroepithelial (NE) cells of the optic lobe (OL) start to differentiate into neuroblasts (NBs), which will
188 subsequently divide to give rise to neurons and glia[15]. We observed that the *clamp* null OL is profoundly
189 reduced in size. The clamp *null* OL neuroepithelia at 120h ALH resemble the 72h ALH control
190 neuroepithelia (i.e., early L3), indicating a likely arrest of the NE optic lobe cells (Figs. 3a, b, e and f).
191 Similarly, the *clamp* mutant central brain (CB) of the mid/late L3, has an underdeveloped morphology and
192 is more similar to the early CB of the control (Figs.3f and a).
193
194 Next, we examined NSCs in *clamp* null and control brains. Full z-stacks of the Dpn-positive NSCs both in
195 the early and mid/late L3 stages (Figs. 3c, d, g and h), revealed that in the *clamp* null NB development both
196 in the CB and OL, is considerably delayed from the early L3 stage and remains so until the mid/late L3
197 stage when the animals die. The OL NB population is greatly affected as the Dpn-positive area at the
198 mid/late L3 stage is much smaller than in controls (Figs 3d and h, dashed outlines). These observations
199 suggest that the deficits observed in brain formation during the L3 stage of the *clamp* null are may be
200 initiated at even earlier developmental stages leading to a dramatic defect in OL development. Interestingly,
201 comparison of early L3 *clamp* heterozygotes ($clamp^{+/-}$) and early L3 *clamp* nulls indicates that a single copy
202 of the *clamp* gene is sufficient to maintain the overall morphology of the developing OL (Supplementary.
203 Fig. 1).
204

205 ***Developmental transcriptomic analysis of clamp null mutants reveals a role for CLAMP in nervous***
206 ***system development***
207
208 The neurodevelopmental deficits observed in the larval *clamp* null mutant brain suggest that the
209 developmental action of CLAMP might initiate at an even earlier developmental stage. As a ubiquitously-
210 expressed TF, CLAMP is present throughout the nervous system from the early embryonic stages due to
211 the deposition of maternal transcripts into the egg[39] (Fig.1a). Each neurodevelopmental stage is
212 characterized by specific transcriptomic events which are controlled by specific TF factor networks[1]. Thus,
213 in order to understand how CLAMP regulates nervous system development on the transcriptomic level, we
214 performed a developmental RNA-sequencing experiment in the *clamp* null mutant during the following key
215 developmental stages: A) the late embryonic stage (16-18 hours), a time point where embryonic
216 neurogenesis pauses[14] and most NBs enter quiescence; and B) larval brains dissected from the mid/late L3
217 stage during which nervous system development in terms of neuronal and glial cell production are at their
218 maximum (see Fig.4a)[40]. Additionally, selection of the specific embryonic time point was based on studies
219 by Haussmann et al. (2008, 2010), where *clamp* was identified as a functional interactor of *elav* and *ewg,*
220 in 16-18h embryos[32, 31].
221
222 GO analysis revealed statistically significant enrichment for developmental/stem cell-related GO
223 categories, including neural development, at both the embryonic and larval developmental stages (Fig.4a).
224 Due to the neurodevelopmental defects in the *clamp* null mutant, we then specifically mined our expression
225 data for differential expression of genes (DEGs) that are implicated in cell cycle attributes, nervous system
226 development and neural stem cell biology. Additionally, we observed enrichment for GO categories
227 involving metabolic pathways. Because post-embryonic neurogenesis is largely orchestrated by signals
228 originating from nutrient availability and insulin signaling[6,41,42], we decided to also mine for metabolism-
229 related DEGs (Fig.4a).
230

231 To evaluate the possibility of direct regulation of DEGs by CLAMP, we determined where CLAMP binding
232 sites are present using FIMO analysis[43]. Previously characterized CLAMP binding motifs were used for
233 this analysis[44]. Interestingly, genes that contain putative CLAMP binding sites and are common between
234 the embryonic and L3 stages include the important proliferation/mitosis regulators *bazooka (baz),*
235 *separation anxiety* (*san)*, a N-terminal acetyltransferase, required for mitotic chromosome segregation[45],
236 *cyclin dependent kinase 7* (*cdk7*), vital for mitosis[46], *PCNA* and *Notch*; *sobremesa* (*sbm*) an SLC7 amino
237 acid transporter expressed in glia and regulating brain development *via* ecdysone signaling[41]; and *Negative*
238 *elongation factor E* (*nelf-E*) (Fig.4e, Embryo and L3 panel).
239
240 Developmental stage-specific genes that contain putative CLAMP binding sites include: A) <u>*Embryo stage*</u>:
241 *anaphase promoting complex subunit 7* (*APC7*)*; pontin (pont)* which is part of the TIP60 complex which
242 regulates NSC attributes*; aurora A (aurA)* a kinase regulating asymmetric protein localization and thus
243 required for NSC proliferation[47]*; extra sex combs (esc)*, a component of the PRC2 complex which regulates
244 NSC proliferation and neural development[48] and *fruitless (fru)*, implicated in the formation of axonal
245 projections in the embryonic CNS[49] (Fig.4e, Embryo panel). B) <u>*L3 stage*</u>: Even more interesting during the
246 L3 stage (Fig.4e, L3 panel), CLAMP binding motifs are found in *gcm,* an essential regulator of glial
247 development*; glass bottom boat* (*gbb*) which regulates both NB proliferation and surface glia survival;
248 tailless (*tll),* a key regulator of optic lobe development and *anaplastic lymphoma kinase (Alk)* which is
249 implicated in cell cycle regulation and NSC proliferation; and *Dichaete* (*D*), a TF regulating neuronal fate
250 in the OL.
251
252 Therefore, CLAMP may be exerting direct control on neural development by affecting the transcription of
253 key players that function in multiple processes including asymmetric cell division, cell cycle and hormone
254 signaling. CLAMP may be directly regulating genes controlling different aspects of neural development in
255 different cell types such a glia (*gcm:* gliogenesis) or NSCs/neuroblasts (*gbb:* expressed in NSCs to control
256 proliferation and SG survival[5]). Therefore, the neurodevelopmental phenotypes observed in the *clamp* null

257 mutant might result from combinatorial changes in diverse signaling cascades originating from different
258 cell types.
259
260 We then proceeded to analyze the individual datasets which revealed that in the *clamp* null embryo, 5917
261 genes were differentially regulated (padj ≤ 0.05, Fig.4b and Supplementary Table 1a). Functional analysis
262 of the DEGs revealed highly statistically-significant enrichment in categories such as cell cycle regulation,
263 cell cycle checkpoints, mitotic cell cycle phase transition, neurogenesis and nervous system development,
264 metabolic processes, synaptic development and signaling (Supplementary Table 1b). We focused our
265 analysis on two major highly enriched GO categories: i). *Cell Cycle Regulation* [GO:0051726, padj: 6.22E-
266 11] and ii). *Nervous System Development* [GO:0007399, padj: 4.32261E-05], due to the fact we identified
267 key genes implicated in both categories as putative direct targets of CLAMP. Specifically, these are genes
268 directly regulating NSC proliferation and division mode: *aurora A (aurA)*, *bazooka* (baz), *pcna* and *notch*
269 *(Fig.4E)*.
270
271 For the *GO:0051726 -Cell Cycle Regulation* category (Supplementary Table 1c), functional analysis of the
272 participating DEGs revealed specific roles including in G2/M transition of mitotic cell cycle, regulation of
273 chromosome segregation, cell cycle G1/S phase transition, negative regulation of nervous system
274 development and of insulin signaling (Fig.4c). These results are in line with CLAMP having direct control
275 over the expression of genes implicated in these processes including, *sbm (Fig.4E)* which is implicated in
276 regulation of neurogenesis through hormone signaling.
277
278 Expression of *elav,* an RNA-binding protein and master regulator of neural development, was increased
279 [L2FC: 0.44; padj: 0.045]. *elav* encodes a protein that regulates the expression of *ewg*. Both elav and *ewg*
280 are critical for nervous system development, and neuronal maturation[50]. Haussmann et al. (2008, 2010)[31,32]
281 reported that *clamp* along with a group of nine functionally-related genes which includes *groucho,* another
282 critical developmental regulator[51], are positively regulated by EWG and restrict synaptic growth (Table 1).

283

284 Analysis of the Haussman et al. (2008) DEGs in the clamp null embryo mRNA-seq data (16-18 hrs),
285 revealed that 9 out of 10 DEGs regulated by ewg are also DEGs in the *clamp* null embryos. Furthermore,
286 the synaptic function-related GO categories were highly enriched in the *clamp* null embryos, as shown for
287 the functionally-related genes that are regulated by *elav* and *ewg*[31,32]. Therefore, it is possible that a
288 synergistic relationship between the CLAMP and the ELAV/EWG pathways exists, in which they regulate
289 each other's expression to assure that brain development occurs normally.

290

291 Meta-analysis of the <u>*GO:0007399: Nervous System development*</u> category (Supplementary Table 1d),
292 revealed strong enrichment in the sub-categories of neurogenesis and central nervous system, visual system
293 development and glial cell development and differentiation (Fig.4d). Some of the DEGs that are part of the
294 *Nervous System development* GO category include: 1) *polo, aPKC, par6, pins, aurA* and *baz* components
295 of the Par-complex which regulates asymmetric neuroblast divisions; 2) *PCNA, RFC38, dacapo,* and *Reptin*
296 (part of the Tip60 complex), which participate in the molecular network controlling cell polarity,
297 asymmetric NSC division and cell fate [52]; 3) *CSN1b, CSN4* and *non-stop* implicated in lamina glia cell
298 migration and optic lobe development [53]. Importantly, *baz* and *pcna* are both candidate direct targets of
299 CLAMP as seen by binding motif analysis (Fig.4E), thus its is highly possible that the enrichment in these
300 categories is the result of direct effects of CLAMP in these key loci.

301

302 Furthermore, several DEGs critical for neural development and NSC biology were identified: *Notch* [L2FC:
303 -0.5, padj: 0.01], *lola* [L2FC: -0.6, padj: 0.004], and components of the Brahma chromatin remodeling
304 complex such as *moira* [L2FC: -1.019, padj: 6.21E-05] [52,54,55]. Importantly, many DEGs are part of specific
305 TF-networks that regulate different aspects of neural stem cell renewal identified by Neumuller et al.
306 (2011): *Su(z)12, Su(var)2-10*, the Hdac1 *Rpd3*, and *lola*. Notch signaling is critical for the balance between
307 proliferation and differentiation in NSCs and it has been suggested that *lola* can have distinct effects on the
308 Notch pathway depending on the expressed *lola* isoform[52]. Moreover, Notch controls neuroblast selection

309 and delamination[56] and is a key regulator of asymmetric divisions throughout the nervous system[57,58].
310 Additionally, Notch maintains the balance between symmetrically and asymmetrically dividing stem cell
311 pools in the optic lobe [59]. Importantly, we have shown that *Notch* may be under direct control by CLAMP
312 (Fig.4E), thus transcriptome changes associated with Notch signaling may be results of the CLAMP-*notch*
313 interaction.
314
315 Categorization of the embryonic DEGs allowed us to identify potential pathways in which CLAMP is likely
316 to regulate target genes. Overall, lack of CLAMP results in dysregulation of three inter-dependent gene/TF
317 networks: 1) neurogenesis/gliogenesis; 2) cell cycle/asymmetric division; and 3) neuronal
318 arborization/synaptogenesis.
319
320 **Transcriptomic analysis of overlapping embryo and L3 *clamp* null DEGs implicates CLAMP in**
321 **regulating embryonic and post-embryonic neurogenesis.**
322
323 The transition from the embryonic to the post-embryonic stage is accompanied by many physiological
324 changes with the most notable being the introduction of feeding which brings about a cascade of metabolic
325 signaling that induces activation of quiescent NSCs and neurogenesis. Comparison of the *clamp* null
326 embryo and L3 mRNA-seq results revealed that a large number of DEGs were shared amongst the two
327 stages (2363 DEGs). (Fig.4b). Meta-analysis of the top two GO categories revealed that the participating
328 genes have roles in nervous system development and neurogenesis, mitotic cell cycle, G protein-coupled
329 receptor signaling pathway and neurotransmitter biosynthesis suggesting a continuum in the roles that
330 CLAMP has in neural development pre- and post-embryonically. These results are in line with the fact that
331 key genes implicated in the above categories are putative direct targets of CLAMP, especially, *baz, pcna*
332 and *notch* and are consistent with the deficits observed in L3 brain development (Figs. 2 and 3).
333

334 The fact that cell cycle-related categories were enriched in our transcriptomic analysis is interesting because
335 CLAMP maintains its expression in L3 proliferating NSCs and co-localizes with PCNA (Figs.1i andj),
336 which has critical roles in the cell cycle[38] and is a candidate direct target of CLAMP. The expression of
337 *pcna* is downregulated in both developmental stages (*clamp* null embryo L2FC: -1.692 and L3 larva L2FC:
338 -0.824, Supplementary Tables 1a and 2a) in addition to cell cycle regulators/chromosome dynamics factors
339 such as *AurB*, *atms, baz, Cdc16,* suggesting that CLAMP regulates cell cycle progression and dynamics
340 directly (Fig.4E) .
341
342 *Clamp* is maternally deposited and its expression is high during the majority of embryogenesis[29] (Fig.1a).
343 While the persistence of maternal *clamp* was not specifically evaluated in late embryos, a study from our
344 lab showed that *clamp* deposited by *clamp* heterozygous mothers persists beyond the embryonic stage and
345 is present in the histone locus body throughout the development of the larval salivary gland [29]. Thus, it is
346 possible that a trace amount of maternally deposited *clamp* could still be present at 16-18 hr embryos.
347
348 **CLAMP regulates genes controlling NSC attributes, glia development and function**
349
350 The L3 stage encompasses a dramatic shift in the establishment of the nervous system. A plethora of
351 signaling pathways, including metabolic signals stimulated by larval feeding[60,42,61], are integrated at the L3
352 stage to allow NSCs to promote maturation of the nervous system. Consistent with this shift in NSC
353 function, GO analysis of the L3 DEGs (Supplementary Table 2b) revealed an enrichment in several broad
354 categories including: neurogenesis, mitotic DNA replication, and neuroblast differentiation. We find
355 changes in many genes critical for nervous system development including those in the following categories:
356 1) neuroblast attributes; 2) cell cycle dynamics; 3) glial cell development; 4) optic lobe development; 5)
357 ecdysone & insulin signaling dynamics; 6) lipid metabolism; 7) Clamp-related interactors; 8) Synapse
358 function & structure.
359

360 Next, we classified DEGs as down-regulated or upregulated in the *clamp* null mutant compared with wild
361 type controls (downregulated vs. upregulated, Tables 2 and 3, respectively). Downregulated genes are genes
362 that are putatively activated by CLAMP in wild type animals. These genes can be classified into the
363 following categories: 1) *NSC attributes* (cell-cycle progression, cell polarity, and survival); 2) *control* of
364 *NSC evolution/differentiation*; 3) *regulation of gliogenesis*; 4) *optic lobe development-specific*. In contrast,
365 upregulated genes that are normally repressed by CLAMP are part of the following categories: 1) *lipid*
366 *metabolism/promoting mobilization of lipids*; 2) *ecdysone and insulin signaling in glia cells*; 3) *pro-*
367 *arborization/synapse formation and function*; 4) *pro-neural/suppression of proliferation*. Based on these
368 data, we hypothesized that loss of *clamp* leads to deficits in neural stem cell attributes and promotes changes
369 that lead to the precocious acquisition of a neuronal fate at the expense of gliogenesis. Our expression data
370 also suggest that loss of CLAMP may cause concomitant activation of lipid metabolism/mobilization as a
371 compensatory response from the stem cell-niche. Additionally, we observed strong downregulation in genes
372 orchestrating OL development such as *eya, tll, dac, optix* (See Table 2 and Supplementary Tables 2d), of
373 which *tll* is a putative direct target of CLAMP (Fig.4E). These results are consistent with the greatly reduced
374 size of the L3 OL (Fig.3) and suggest a greater sensitivity of OL NSCs to the absence of CLAMP compared
375 with the rest of the brain.
376
377 ***CLAMP promotes NSC proliferation and prevents precocious neurogenesis***
378
379 Our developmental transcriptomic analysis lead us to hypothesize that CLAMP regulates neural stem
380 cell/neuroblast attributes, progeny fate and synaptic circuit formation (axonogenesis, synaptogenesis). For
381 example, lack of CLAMP leads to a downregulation of genes that regulate neural stem cell stemness and
382 cell cycle progression both in embryos and larvae (Figs.4c-e). Therefore, we hypothesized that lack of
383 CLAMP promotes precocious neurogenesis at the expense of glia formation through the L3 stage. To test
384 our hypothesis that CLAMP regulates neural stem cell proliferation, we evaluated mid-late L3 brains for
385 proliferating NSCs using the S-phase marker EdU and the NSC marker Dpn. In agreement with our initial

386 observations (Fig.3), the OL in *clamp* null larvae brains was dramatically reduced in size compared to
387 controls, and both the CB and OL contained fewer proliferating NSCs ($EdU^{+}Dpn^{+}$, Figs.5a and c and
388 Supplementary Figs.2 a, b). Quantification of total proliferating NSCs throughout the CNS yielded a
389 dramatic ~90% reduction compared to controls (Fig. 5e). Moreover, the total number of proliferating cells
390 was reduced compared to controls, suggesting a reduced proliferation of stem cells and/or change in cell
391 cycle dynamics in the absence of CLAMP (EdU+ Fig.5e).
392
393 Genes encoded by many pro-neural TFs are upregulated in the absence of CLAMP (Table 3), in addition
394 to TFs that promote cell cycle regulation in proliferating stem cells. Specifically, in the L3 *clamp* null brain
395 the *Dpn* transcript, which regulates NSC proliferation, was significantly reduced (Table 2; L2FC: -0.665,
396 padj: 0.00245). Reduction in *Dpn* transcript levels correlates with the reduced numbers of proliferating
397 NSCs in the *clamp* null and suggests that neuron production may be altered in the absence of *clamp*. The
398 TF Prospero (Pros), acts as a master regulator driving the decision of stem cells to either self-renew or
399 differentiate[62], while nuclear presence of Pros signals the initiation of neuronal differentiation[62,63]. Thus, to
400 evaluate changes in neuronal production in the *clamp* null brain we performed Pros staining. We found
401 that the *clamp* null brain contained more clusters of nuclear Pros than matched controls, thus indicating a
402 rapid change in NSC cell fate attributes[64] (Figs.5b and d, arrows indicate Pros+ clusters). Interestingly,
403 while the total number of NSCs in the *clamp* null brain was reduced by approximately 70% (Dpn^{+}, Fig.5f),
404 Pros+ cell numbers were increased by approximately 70% ($Pros^{+}$, Fig.5f), indicating that stem cells are
405 acquiring a precocious neuronal fate. The reduction in NSCs is particularly evident in the OL, where very
406 few Dpn+ cells were observed and instead many Pros+ cells were present (Figs.5a and c- dashed lines and
407 outlines in Figs.5b and d indicate the OL). Pros, acts a transcriptional repressor of self-renewal genes and
408 induces differentiation[47]. In the *clamp* null brains, a significantly lower number of cycling stem cells have
409 nuclear Pros (Pros+EdU+, Sup.Fig.2c), suggesting that in the absence of CLAMP, neural stem cells either
410 undergo fewer cell division cycles and/or exit the cell cycle to acquire a precocious differentiated fate.
411

412 To further evaluate changes in the neuronal pool we performed Elav staining to label neurons[65] which
413 revealed that *clamp* null brains contained a higher density of Elav$^+$ clusters compared to controls (Figs.5g
414 and h). However, even though the overall Elav+ cluster density increased the Elav$^+$ zone in the OL was
415 reduced compared to controls (Figs. 5g and h, yellow outlines). Immunostaining with the apoptotic marker
416 Dcp1 revealed increased and specific presence of Dcp1$^+$ nuclei in the OL in *clamp* nulls, compared to the
417 controls which instead had more widespread apoptosis (Figs. 5i and j). Moreover, in more dorsal optical
418 sections big Dcp1+ clusters were visible in the medulla and lamina area (Supplementary Figs.3a and b).
419 These results suggest that in the absence of CLAMP a pro-differentiation pathway is activated in stem cells
420 at the expense of their self-renewal which especially impacts the OL.
421
422 ***Lack of CLAMP results in reduction in number of surface glia and increased lipid droplet concentration***
423
424 OL development is highly dependent on glia-neuron interactions because glia form a supportive niche for
425 neural stem cells to function[13,66]. Our transcriptomic analysis supports the hypothesis that lack of CLAMP
426 promotes neuronal differentiation at the expense of gliogenesis from the late embryo stage. Furthermore,
427 the TF master regulator of gliogenesis, *gcm*, is a putative CLAMP target (Fig.4e).
428
429 Therefore, the defects observed in OL development of the L3 *clamp* null are likely to be the combinatorial
430 result of deficits in glia formation and precocious neurogenesis. It was recently shown that surface glia (SG)
431 are required for NB proliferation[67] using two different mechcanisms: 1) SG regulate NSC proliferation *via*
432 the secretion of the proteoglycan Dally-like, (Dlp)[5]; 2) Stem cells secrete the BMP-ligand Glass bottom
433 boat (Gbb) which regulates both their proliferation and survival. Furthermore, *gbb* is a putative direct
434 transcriptional target for CLAMP (Fig.4e) because it contains CLAMP binding sites and is downregulated
435 in the *clamp* null L3 brains (Supplementary Table 2d). Also, we observed enrichment of the BMP-signaling
436 GO category in the *clamp* null (Fig.4d). Therefore, it is also possible that the effects we see on neural
437 development in the *clamp* null brains are the result of changes in the dynamics between SG and NSCs. To

438 investigate this possibility, we used the glia-specific marker Repo to mark glial cells and we counted SG in
439 L3 brains (Ref Avet-Rochex) [40]. This approach revealed that the SG number in the *clamp* null was reduced
440 by ~25 % compared to the control (Figs.6 a-d). In addition to changes in SG, we observed that the
441 distribution and numbers of glia throughout the brain and especially in the OL exhibited a different
442 morphology within the lobula plug (Supplementary Figs. 3c-f). Overall, these data suggest that CLAMP
443 specifically regulates gliogenesis and glia distribution especially in the OL.
444
445 To determine if the effect on SG numbers was due to the lack of CLAMP in glia specifically, we used the
446 GAL4-UAS system to induce *clamp*-RNAi knock down (KD) using the glia-specific driver, *repo-GAL4*[68].
447 Interestingly, we find that in the *repo>clamp RNAi* brains, the number of SG was reduced to a similar extent
448 as in the *clamp* nulls (Repo+, Figs. 6a-d). To determine whether glia-specific or neuronal-specific *clamp*
449 depletion has differential effects on the proliferation (EdU+) and the number of NSCs (Dpn+ cells), we also
450 performed neuronal *clamp* KD by crossing to an *elav-GAL4* fly line[69]. Comparison with the data we already
451 obtained from the *clamp* null and control brains (see Figs.5e and f) revealed that *clamp* KD in neuronal
452 lineages did not result in significant changes either in EdU+ or Dpn+ cells, glia-specific *clamp* KD caused
453 a reduction in the number of total proliferating cells (EdU+). Therefore, glial CLAMP regulates
454 proliferation of NSCs likely *via* both cell autonomous mechanisms (e.g., reduction in Dpn+ gliogenic
455 NSCs) and *via* non-cell autonomous mechanisms (regulation of proliferation by niche glia).
456
457 ***Lack of CLAMP causes an imbalance in NSC niche homeostasis***
458
459 One mechanism by which the NSC niche protects the stem cells from environmental stressors like hypoxia
460 and oxidative stress is by the mobilization of polyunsaturated fatty acids away from lipid membranes and
461 into lipid droplets (LDs) formed by cortex and subperineural glia cells (SPG). The GO analysis of the L3
462 *clamp* null transcriptomic data (Supplementary Table 2b) showed that the category metabolic process
463 (GO:0008152) was amongst the most enriched, and genes implicated in lipid metabolism were significantly

464 upregulated (Sup.Table 2c). Additionally, both *sbm* and *wunen (wun),* genes regulating neural development
465 *via* hormone signaling and regulation of lipid levels respectively, are both putative direct targets of CLAMP
466 (Fig.4E) which are upregulated in the L3 *clamp* null brains (Table 3). Therefore, we hypothesized that in
467 the absence of CLAMP, the niche lipid droplet formation mechanism is activated.
468
469 To test this hypothesis, we quantified LDs following staining with the neutral lipid-specific dye LipidTOX.
470 We found that the concentration of LDs was increased by 50% in the *clamp* null brain compared to controls
471 (Figs.6j-p). Also, the distribution of LDs in the *clamp* null brain differed compared to control brains.
472 Interestingly, large LD formations were observed surrounding dividing NBs in the *clamp* null more often
473 than in the control brain (Figs.6l and m and Supplementary.Fig.4). Collectively these results suggest that
474 despite the lack of CLAMP causing a reduction in LD-producing SG, the remaining SG cells undergo lipid
475 mobilization and increase LD formation, perhaps in an attempt to save the remaining proliferating NSCs.
476
477 In recent years, LD biology and function has been gaining traction in the context of both basic biology and
478 disease because LDs have proven to be critical and plastic organelles that actively participate in various
479 cellular functions[70]. An intriguing observation is the function of LDs as a storage location for free histones,
480 which in turn affects mitotic chromosome structure. Specifically, interactions between the LD-surface-
481 located Invadolysin and the SAGA chromatin modifying complex regulate chromosome structure[71-73]. The
482 GO analysis of the L3 stage transcriptomic data indicated a deficit in the neuroblast division mechanism
483 and in chromosomal organization (See Supplementary Table 2b and Table 2). Additionally, critical
484 regulators of asymmetric NSC division and mitotic spindle orientation were significantly down-regulated
485 in the *clamp* null brain (see Table 2) and some were identified as putative CLAMP targets both at the
486 embryo and L3 stage (Fig.4e).
487
488 Based on the connection between LDs and chromosome behavior and the results from our *clamp* null L3
489 RNA-seq, we decided to check for morphological differences in mitotic neuroblast chromosomes from

490 *clamp* null brains. Interestingly in mitotic chromosome preparations from *clamp* null brains, we observed
491 hyper-condensed, "snowflake-like" chromosome formations in contrast to the elongated and well separated
492 chromosomes observed in in control preparations (Figs.7a-d, yellow outlines). Occasionally, in the *clamp*
493 null preparations we would observe chromosomes with normal morphology, but this was less common
494 (Fig.7d, magenta outline). Co-staining with the differentiation marker Pros, also revealed the presence of
495 more nuclei positive for Pros in contrast to controls (Fig.7a and b,) supporting the observations reported in
496 Fig.5 (whole brain images) in which we observed precocious neuronal differentiation in the absence of
497 CLAMP. Moreover, in the null preparations we see fewer cells expressing Dachshund (Dac) which
498 regulates OL development (Figs.7c and d) and an overall decrease in cell size compared to controls.
499
500 In summary, these results suggest that lack of CLAMP affects neurogenesis at multiple levels, from
501 impacting mitotic chromosomal structure to affecting the neural stem cell niche homeostasis which leads
502 to precocious differentiation of neural stem cells.
503
504 **Discussion**
505
506 The understanding of the molecular and transcriptional mechanisms by which neural stem cells function to
507 ultimately build the brain is critical both to understand how brains develop. Signaling relays originating
508 from the stem niche play an instructive role in the neurogenetic process and highlight the fact that the
509 environmental context acts as an additional layer in addition to intrinsic developmental signals[2,3]. In this
510 study, we have defined a new role for the essential transcription factor, CLAMP, in nervous system
511 development and NSC-niche interactions. Specifically, we show that CLAMP is important both for
512 neuronal and glial cell generation and regulates NSC function *via* cell-intrinsic and NSC niche-dependent
513 mechanisms that implicate niche glia.
514

515 Neural development and NSC function are intricately linked to niche glia and depend on support and
516 nutrition from surface glia *via* Gbb-Dlp signaling, which sustains NSC proliferation and survival but also
517 ensures the survival of surface glia[5]. Thus, there is an interdependency between NSCs and niche glia,
518 ensuring overall homeostasis in the stem cell niche. In *clamp* null and *repo>clamp* RNAi larvae brains,
519 surface glia numbers are reduced to the same extent indicating that lack of glial CLAMP affects gliogenesis
520 (Fig.6d). Furthermore, the glial master gene, *gcm,* contains CLAMP binding motifs, indicating that CLAMP
521 is likely to directly regulate gliogenesis (Fig.4e).
522
523 In the post-embryonic nervous system, *gcm* and *gcm2* are expressed in OL NSCs destined both for glia and
524 neuron generation which they regulate *via* downstream mechanisms involving Dachshund (Dac)[79], a gene
525 whose expression is reduced in the *clamp* null (Table 2 and Fig.7d). Moreover, both *gcm* and *gcm2*
526 transcript levels were greatly reduced in the *clamp* null L3 brain and *gcm* contains CLAMP binding sites
527 (Fig.4e). The OL contains a special population of NSCs which generate both glia and neurons (Lawfs),
528 from a common progenitor population under the control of Notch signaling[80]. Moreover, Notch is a key
529 regulator which maintains the balance between symmetric/self-renewing and asymmetric NSCs divisions;
530 loss of Notch function promotes precocious differentiation and premature neurogenesis [59]. In the absence
531 of CLAMP, *Notch* is at least two-fold downregulated both in the embryonic and L3 stages (Supplementary
532 Table 1a and Table 2), and we determined that Notch has a nearby CLAMP binding site (Fig.4e). Overall,
533 our data support a model in which CLAMP directs *Notch* and *gcm* signaling to regulate NSC proliferation
534 and differentiation.
535
536 The formation of the OL was profoundly impaired in the *clamp* null, a phenotype accompanied by reduction
537 of EdU^+ NSCs (Figs.5a-d). We also observed increased numbers of $Pros^+$ cells in the null OL (Figs. 5b and
538 d, outlined area) and throughout the brain, consistent with lack of CLAMP promoting a neurogenic over a
539 gliogenic fate. While glial *clamp* KD results in a partial reduction in the number of proliferating NSCs
540 (EdU^+, Fig.6e), it does not affect the number of Dpn^+ NSCs/neuroblasts. These results suggest an effect on

541 the Dpn$^-$ progeny of the NSCs such as the ganglion mother cells (GMCs). Also, it is possible that there are
542 changes in the cell cycle kinetics that cause fewer NSCs to be actively proliferating. This possibility is
543 consistent with the GO analysis which identified genes involved in cell cycle kinetics/transitions (Fig4.c).
544 Moreover, CLAMP may have a regional role in OL neurogenesis because *tll* is a candidate direct target for
545 CLAMP (Fig.4) and other transcription factors critical for OL neurogenesis such as *eya, dac* and *optix* are
546 downregulated (see Table 2).
547
548 Under conditions of hypoxia and oxidative stress, niche glia form lipid droplets in order to reduce reactive
549 oxygen species and inhibit oxidation of polyunsaturated fatty acids that will damage both the NSCs and
550 glia[6]. In the *Drosophila* larval brain lipid droplets are formed exclusively by glial cells and not neurons,
551 and specifically by subperineural and superficial cortex glial cells, with the latter most enriched [21]. Cortex
552 glia are a very unique glial population. At the initiation of postembryonic neurogenesis, cortex glia ensheath
553 each dividing neuroblast and their membrane acquires the appropriate morphology to accommodate the
554 proliferating neuroblast and its progeny. Thus, these cells provide spatial organization for each NSC
555 progeny cell, while at the same time nurturing and protecting NSCs [5,21] . In the absence of CLAMP, there
556 is a marked increase in the levels of brain LDs (Figs.6j-p) concomitant with the changes in NSC and surface
557 glia numbers.
558
559 Thus, loss of CLAMP could be triggering a compensatory mechanism in glia through increase of lipid
560 formation and/or abnormal lipid storage in glia based on our transcriptomics which showed enrichment for
561 genes and GO categories implicated in insulin signaling, lipid mobilization and metabolism (Table 3 and
562 Fig.4). Moreover, *wunen (wun)* a membrane-localized lipid phosphate phosphatase which regulates the
563 levels of bioactive lipids and is expressed in SPG[81,82] is a putative direct target of CLAMP (Fig.4e) which
564 is upregulated in *clamp* nulls (Table 3). Thus, it is also possible that lack of CLAMP results in abnormal
565 accumulation of LDs in surface glia through *wun* regulation. In the *clamp* null L3 brain there is also a
566 dramatic upregulation in the levels of the glial-derived *dilp6*. dIlps- insulin-like peptides are released by

567 blood–brain barrier glial cells and act *via* the insulin/insulin-like growth factor pathway. Specifically dIlp6
568 activates the PI3K/Akt pathway in NSCs to promote their reactivation[8,60]. We noted an enrichment of
569 differentially expressed genes which were part of the insulin signaling pathway (Fig.4c) such as *dIlp6* and
570 upregulation and reduction in transcription of genes regulating cell cycle progression. Therefore, that lack
571 of CLAMP results in impairment of NSC progression through the cell cycle/exit from quiescence, and thus
572 stimulates a compensatory response from the NSC niche to overcome it.
573
574 Interestingly, we observed that large LDs are more often found around dividing neuroblasts in the *clamp*
575 null brains (Figs.6l and m; Supplementary Fig.4). Also, NSCs lacking CLAMP show abnormal
576 chromosomal behavior in larval mitotic chromosome preparations (Fig.7). During neuroblast divisions, the
577 axis of polarity is regulated by intrinsic and external cues from the daughter GMC which induces
578 polarization of the dividing NSC in order to orient its axis of polarity and its division plane[83]. Loss of the
579 proper orientation reduces the contact surface area with cortex glia and thus renders the proliferating NSC
580 more sensitive to stress. Lack of CLAMP results in downregulation of the mitotic polarization determinants
581 including *baz,* which is putatively under CLAMPs transcriptional control (Fig.4e). Therefore, the axis of
582 polarity may be disrupted in *clamp* nulls which reduces the area of contact between cortex glia ensheathing
583 the NSC. In budding yeast, the storage of excess lipids in LDs during anaphase is critical for proper
584 cytokinesis and cell division and disruption of this process leads to defects in cell separation[84]. Furthermore,
585 accumulation of LDs was shown to be important for the progression of the cell cycle and proliferation in
586 human cancer cells[85]. Therefore, it is possible that the formation of large LDs around diving neuroblasts in
587 the *clamp* null is yet another compensatory mechanism that niche glia uses to ensure proper division of
588 NSC.
589
590 We also observed that the *foxO* gene (Forkhead box, class O) is part of many of the cell cycle sub-categories
591 that we identified from GO analysis, including the *insulin signaling category*, which is a known target of
592 FOXO [74]. FOXO belongs to a family of highly dynamic and conserved transcription factors and regulates

593 gene expression during processes such as apoptosis, cell-cycle transitions including negative regulation of
594 G1/S and G2/M [75], both of which are highly enriched in our GO analysis. Overexpression of FOXO during
595 larval development results in reduction both in cell size and number in the developing eye [74]. In addition, it
596 was shown that FOXO affects the temporal sequence and cell fate specification in a subset of olfactory
597 neurons in *Drosophila* [76]. Interestingly, in the *clamp* null embryo the *foxO* transcript is upregulated (L2FC:
598 0.46846, padj:0.000283, Supplementary Table 1a). Moreover, glia-derived DILP6 activates the Insulin
599 Receptor (InR) on cholinergic neurons and induces Jeb activation which acts downstream to regulate FoxO
600 activity in Insulin Producing Cells (IPCs) [68,69]. Therefore, it is possible that some of the phenotypic effects
601 that we observed in the *clamp* null mutant are related to dysregulation of *foxO* gene expression [74,76] .
602
603 Glial cells can arise from different mechanisms, either from dedicated glioblasts or from NBs that have
604 both glial and neuronal potential[86-89]. Our results indicate that CLAMP is important both for maintaining
605 the proliferation of NSCs by acting in a cell-type specific manner (i.e, glia vs. NSCs) and in a cell-intrinsic
606 mechanism that implicates regulation of chromosomal behavior and fate determinants such as *gcm* and
607 *Notch*. In addition, CLAMP acts *via* niche-dependent mechanisms that implicate surface glia, Dilp6/insulin
608 signaling and lipid droplet formation. Overall, here we have shown that CLAMP is an important regulator
609 of NSC differentiation and of the stem cell niche.
610
611
612
613
614
615
616
617
618

619 ***Materials and Methods***

620

621 ***Fly Strains***

622

623 Fly stocks used in this study were as follows: y^1w^1 (maintained in the Larschan lab); *clamp* null and *clamp*
624 rescue lines, both of which have been generated by Urban et al.(2017) and described therein [25]. Briefly, the
625 *clamp* null, is a CRISPR-Cas9 generated frameshift mutation which abolishes CLAMP protein expression,
626 whereas, the *clamp* rescue was generated by introduction of a full *clamp* rescue construct on chromosome
627 3L. For the RNAi experiments the following lines were used: *repo-GAL4*, *elav*^{c155} (*elav-GAL4*) and UAS-
628 *clamp-RNAi,* all obtained from the Bloomington Stock Center. All crosses were done at 25ºC and a 12-hour
629 light/dark cycle.

630

631 ***Immunostaining***

632

633 The following antibodies were used: Rabbit anti-CLAMP (1:200, Abcam custom made), mouse anti-Repo
634 (1:50, Developmental Studies Hybridoma Bank (DSHB) 8D12), rabbit anti-DCP1 (1:100, Cell Signaling),
635 rat anti-Deadpan (Dpn, 1:100, Abcam), rat anti-Elav (1:50, DSHB), mouse anti-Prospero (Pros, 1:30,
636 DSHB), mouse anti-Dachshund (Dac, 1:40, DSHB), PCNA (PC10, Abcam), Nc82 (1:10, DSHB).
637 Secondary antibodies used were Alexa Fluor Conjugated A405, A488, A568, A647 (1:1000, Invitrogen).
638 A standard staining protocol was used.

639

640 ***Quantification of glia***

641

642 To quantify superficial glia, 3-µm projections (z-projections of three 1-µm optical sections) of the dorsal
643 surface of third instar larval brain hemispheres stained for Repo were used and quantified manually using
644 Adobe Photoshop. Six hemispheres were quantified for each genotype.

645 ***Image acquisition and processing***

646

647 Fluorescent images were acquired using an inverted Olympus FLUOVIEW FV1000 confocal laser
648 scanning microscope. Adobe Photoshop was used to adjust brightness and contrast in images and ImageJ
649 (or Fiji (Schindelin et al., 2012)) was used to analyzed images while Adobe Illustrator was used to compile
650 figures.

651

652 ***EdU Incorporation***

653

654 EdU incorporation in proliferative brain cells, was performed using Click-It Edu Alexa Fluor A488
655 (Thermo Fisher Scientific, MA, USA) in an adaptation of Tastan and Liu (2015)[90] method. Briefly, samples
656 were dissected in ice-cold Graces media and then transferred in Graces media containing 5µg/ml of EdU,
657 for 2 hours at room temperature. Then, samples were washed in 0.1% PBST and fixed in 4% PFA in 0.1%
658 PBST, for 20 min at room temperature. Following, tissues were washed in 5% HINGS in 0.1 % PBST and
659 then permealized in 0.5% PBST for 20 min (RT). After this step, the EdU Click It steps were followed
660 according to the manufacturer's instructions and then additional antibody staining was followed as
661 described above.

662

663 ***Brain Lipid Staining***

664

665 Neutral brain lipids were stained using the LipidTOX dye as described in Bailey et al. (2015) [6]. Briefly,
666 tissue was dissected in ice-cold PBS, and fixed overnight in 2% PFA in phosphate buffer with lysine at
667 room temperature. Following PBS washes, the samples were permealized in 0.2% PBST, and stained with
668 DAPI. Then followed LipidTOX Red (1:1000) staining with overnight incubation. Following PBS washes,
669 samples were mounted in ProLong Gold for imaging.

670

671 ***Larval Staging***

672

673 Third Instar larvae crawling on the vial walls were selected to be mid/late stage using the bromophenol blue
674 method adjusted from Maroni and Stamey (1983) [91], using 0.05% w/v bromophenol blue-containing fly
675 food. To control for variations in brain size due to crowding, experiments were done under controlled
676 density conditions. Specifically, a set number of mated males and females were allowed to mate for 5 hours
677 and then removed from the vial. Additionally, the progeny number was evaluated to validate that we did
678 not have large deviations between control and *clamp* mutant larvae numbers.

679

680 ***RNA extraction and RNA sequencing***

681

682 Mid/late third instar larvae were staged using the bromophenol blue method and larval brains were dissected
683 in ice-cold PBS, collected in TRIzol until RNA extraction was performed using the phenol-chloroform
684 method. Each biological replicate was generated by pooling at least 12 larval brains. mRNA-focused
685 sequencing libraries were constructed from total RNA using the Illumina Truseq RNA Library kit v2
686 according to the manufacturer's instructions (no strand-information). Paired-end 100 bp or 50 bp was
687 performed on an Illumina HiSeq2500 sequencer in High-Output mode at the MGH NextGen Sequencing
688 Core. Four biological samples were used per experimental condition.

689

690 ***RNA sequencing data analysis and Differential Gene Expression Analysis***

691

692 RNA-seq reads were processed using FastQC[92] with default parameters to check the quality of raw sequence
693 data and filter out sequences flagged for poor quality, and aligned using HISAT2[93] . Then read counts per
694 gene were generated via HTSeq[94] using the *Drosophila melanogaster* genome dm6 (BDGP6) genome as
695 reference. Differential gene expression analysis was performed using DESeq2[95]. *gProfiler* was used for GO
696 analysis [96]. Using TIMEOR[97] the temporally differentially expressed genes where displayed in interactive

697 expression clustermaps along the developmental time scale (see Supplementary files: *Embryo_heatmap* and
698 *L3_brain_heatmap*), from which additional, GO analysis was performed by TIMEOR *via* clusterProfiler[98]
699 to evaluate for possible gene networks.
700
701 ***Clamp Binding motifs***
702
703 We used FIMO[43] to identify individual CLAMP motif occurrences within ±1KB from the transcription
704 start and end sites for all genes within each gene trajectory cluster. The position weight matrix used[44]
705 highlights the CLAMP motif independently of GAF binding potential. The specific command used is: *(fimo*
706 *--oc $OUTPUT_DIR/ CLAMP_PWM.txt $geneList)*
707
708 ***Western Blotting***
709
710 Larval brains were dissected from wandering third instar larvae in ice-cold 0.7% saline and transferred in
711 PBS + 0.3% Triton X-100 on ice. Liquid was carefully removed, then samples were frozen in liquid
712 nitrogen and stored at -80°C until use. Approximately ten brains were collected per biological replicate.
713 For protein extraction, 50 µL of ice-cold RIPA buffer (150 µL1M Tris-HCl pH 8, 12 µL 0.5M EDTA, 0.003
714 g sodium deoxycholate, 15 µL 20% SDS, 90 µL 5M NaCl, 30 µL 50x protease inhibitor, and 2700 µL
715 water) was added to each sample. Samples were homogenized using an electric handheld homogenizer and
716 disposable plastic pestle. After homogenization, the pestle was rinsed with an additional 50 µL of RIPA for
717 a total volume of 100 µL per tube. Samples were rotated at 4°C for 1-2 hours. Protein concentration was
718 quantified using the Qubit Protein Assay kit (Thermo Fisher Scientific).
719
720 ***Statistical Analysis***
721

722 Excel and GraphPad Prism were used for statistical analysis. Bar graphs were generated using the mean
723 and standard error of the mean (SEM) for each sample. Statistical significance was determined using an
724 unpaired Student's t-test.
725
726 ***Materials & Correspondence***
727
728 Data and materials generated in this study are available upon request from the corresponding authors.
729 Transcriptomic data have been deposited in Gene Expression Omnibus (GEO) Database, under the
730 accession number GSE148704.
731
732
733
734
735 REFERENCES
736

737 1 Konstantinides, N. *et al.* Phenotypic convergence: distinct transcription factors regulate common
738 terminal features. *Cell* **174**, 622-635. e613 (2018).
739 2 Scadden, D. T. The stem-cell niche as an entity of action. *Nature* **441**, 1075-1079 (2006).
740 3 Speder, P. & Brand, A. H. Systemic and local cues drive neural stem cell niche remodelling during
741 neurogenesis in Drosophila. *Elife* **7**, e30413 (2018).
742 4 Dani, N. *et al.* A cellular and spatial map of the choroid plexus across brain ventricles and ages.
743 *BioRxiv*, 627539 (2019).
744 5 Kanai, M. I. *et al.* Regulation of neuroblast proliferation by surface glia in the Drosophila larval
745 brain. *Scientific reports* **8**, 1-15 (2018).
746 6 Bailey, Andrew P. *et al.* Antioxidant Role for Lipid Droplets in a Stem Cell Niche of Drosophila.
747 *Cell* **163**, 340-353, doi:https://doi.org/10.1016/j.cell.2015.09.020 (2015).

748 7 Yuan, X., Sipe, C. W., Suzawa, M., Bland, M. L. & Siegrist, S. E. Dilp-2–mediated PI3-kinase
749 activation coordinates reactivation of quiescent neuroblasts with growth of their glial stem cell
750 niche. *Plos Biology* **18**, e3000721 (2020).
751 8 Spéder, P. & Brand, A. H. Gap junction proteins in the blood-brain barrier control nutrient-
752 dependent reactivation of Drosophila neural stem cells. *Dev Cell* **30**, 309-321 (2014).
753 9 Ramon-Cañellas, P., Peterson, H. P. & Morante, J. From early to late neurogenesis: Neural
754 progenitors and the glial niche from a fly's point of view. *Neuroscience* **399**, 39-52 (2019).
755 10 Hindle, S. J. & Bainton, R. J. Barrier mechanisms in the Drosophila blood-brain barrier. *Frontiers*
756 *in neuroscience* **8**, 414 (2014).
757 11 Hartenstein, V. & Campos-Ortega, J. A. Early neurogenesis in wild-typeDrosophila melanogaster.
758 *Wilhelm Roux's archives of developmental biology* **193**, 308-325 (1984).
759 12 Prokop, A. & Technau, G. M. The origin of postembryonic neuroblasts in the ventral nerve cord of
760 Drosophila melanogaster. *Development* **111**, 79-88 (1991).
761 13 Ramon-Cañellas, P., Peterson, H. P. & Morante, J. From early to late neurogenesis: Neural
762 progenitors and the glial niche from a fly's point of view. *Neuroscience* (2018).
763 14 Hakes, A. E., Otsuki, L. & Brand, A. H. A newly discovered neural stem cell population is
764 generated by the optic lobe neuroepithelium during embryogenesis in *Drosophila melanogaster*.
765 *Development* **145**, dev166207, doi:10.1242/dev.166207 (2018).
766 15 Contreras, E. G., Sierralta, J. A. & Oliva, C. Novel strategies for the generation of neuronal
767 diversity: lessons from the fly visual system. *Frontiers in Molecular Neuroscience* **12**, 140 (2019).
768 16 Egger, B., Chell, J. M. & Brand, A. H. Insights into neural stem cell biology from flies.
769 *Philosophical Transactions of the Royal Society B: Biological Sciences* **363**, 39-56 (2008).
770 17 Gallaud, E., Pham, T. & Cabernard, C. in *Asymmetric Cell Division in Development, Differentiation*
771 *and Cancer* 183-210 (Springer, 2017).
772 18 Crews, S. T. Drosophila Embryonic CNS Development: Neurogenesis, Gliogenesis, Cell Fate, and
773 Differentiation. *Genetics* **213**, 1111-1144, doi:10.1534/genetics.119.300974 (2019).

774 19 Yildirim, K., Petri, J., Kottmeier, R. & Klämbt, C. Drosophila glia: Few cell types and many
775 conserved functions. *Glia* **67**, 5-26 (2019).
776 20 Sousa-Nunes, R., Yee, L. L. & Gould, A. P. Fat cells reactivate quiescent neuroblasts via TOR and
777 glial insulin relays in Drosophila. *Nature* **471**, 508-512 (2011).
778 21 Kis, V., Barti, B., Lippai, M. & Sass, M. Specialized cortex glial cells accumulate lipid droplets in
779 Drosophila melanogaster. *PLoS One* **10**, e0131250 (2015).
780 22 Morante, J., Vallejo, D. M., Desplan, C. & Dominguez, M. Conserved miR-8/miR-200 defines a
781 glial niche that controls neuroepithelial expansion and neuroblast transition. *Dev Cell* **27**, 174-187
782 (2013).
783 23 Soruco, M. M. *et al.* The CLAMP protein links the MSL complex to the X chromosome during
784 Drosophila dosage compensation. *Genes Dev* **27**, 1551-1556, doi:10.1101/gad.214585.113 (2013).
785 24 Larschan, E. *et al.* Identification of chromatin-associated regulators of MSL complex targeting in
786 Drosophila dosage compensation. *PLoS Genet* **8**, e1002830, doi:10.1371/journal.pgen.1002830
787 (2012).
788 25 Urban, J. A., Doherty, C. A, Jordan, W. T, Bliss, J. E, Feng, J., Soruco, M. M, Rieder, L. E, Tsiarli,
789 M. A, Larschan, E. N. The essential Drosophila CLAMP protein differentially regulates non-coding
790 roX RNAs in male and females. *Chromosome Research* **25**, 101-113 (2017).
791 26 Soruco, M. M. *et al.* The CLAMP protein links the MSL complex to the X chromosome during
792 Drosophila dosage compensation. *Genes & development* **27**, 1551-1556 (2013).
793 27 Tikhonova, E. *et al.* The simultaneous interaction of MSL2 with CLAMP and DNA provides
794 redundancy in the initiation of dosage compensation in Drosophila males. *Development* **146**,
795 dev179663 (2019).
796 28 Kaye, E. G. *et al.* Drosophila dosage compensation loci associate with a boundary-forming
797 insulator complex. *Molecular and cellular biology* **37**, e00253-00217 (2017).
798 29 Rieder, L. E. *et al.* Histone locus regulation by the Drosophila dosage compensation adaptor protein
799 CLAMP. *Genes & development* **31**, 1494-1508 (2017).

800 30 Urban, J. *et al.* Enhanced chromatin accessibility of the dosage compensated Drosophila male X-
801 chromosome requires the CLAMP zinc finger protein. *PloS one* **12**, e0186855 (2017).
802 31 Haussmann, I. U., White, K. & Soller, M. Erect wing regulates synaptic growth in Drosophila by
803 integration of multiple signaling pathways. *Genome biology* **9**, R73 (2008).
804 32 Haussmann, I. U. & Soller, M. Differential activity of EWG transcription factor isoforms identifies
805 a subset of differentially regulated genes important for synaptic growth regulation. *Dev Biol* **348**,
806 224-230, doi:10.1016/j.ydbio.2010.09.006 (2010).
807 33 Brown, J. B. *et al.* Diversity and dynamics of the Drosophila transcriptome. *Nature* **512**, 393-399
808 (2014).
809 34 Graveley, B. *et al.* The D. melanogaster transcriptome: modENCODE RNA-Seq data for dissected
810 tissues. *Retrieved from website: http://www. modencode. org/Celniker. shtml* (2011).
811 35 Thurmond, J. *et al.* FlyBase 2.0: the next generation. *Nucleic acids research* **47**, D759-D765
812 (2019).
813 36 Schonenberger, F., Deutzmann, A., Ferrando-May, E. & Merhof, D. Discrimination of cell cycle
814 phases in PCNA-immunolabeled cells. *BMC Bioinformatics* **16**, 180, doi:10.1186/s12859-015-
815 0618-9 (2015).
816 37 Zerjatke, T. *et al.* Quantitative cell cycle analysis based on an endogenous all-in-one reporter for
817 cell tracking and classification. *Cell reports* **19**, 1953-1966 (2017).
818 38 Kurki, P., Vanderlaan, M., Dolbeare, F., Gray, J. & Tan, E. Expression of proliferating cell nuclear
819 antigen (PCNA)/cyclin during the cell cycle. *Experimental cell research* **166**, 209-219 (1986).
820 39 Rieder, L. E., Jordan, W. T. & Larschan, E. N. Targeting of the Dosage-Compensated Male X-
821 Chromosome during Early Drosophila Development. *Cell Reports* **29**, 4268-4275.e4262,
822 doi:https://doi.org/10.1016/j.celrep.2019.11.095 (2019).
823 40 Avet-Rochex, A., Kaul, A. K., Gatt, A. P., McNeill, H. & Bateman, J. M. Concerted control of
824 gliogenesis by InR/TOR and FGF signalling in the Drosophila post-embryonic brain. *Development*
825 **139**, 2763-2772, doi:10.1242/dev.074179 (2012).

826 41 Galagovsky, D. *et al.* Sobremesa L-type amino acid transporter expressed in glia is essential for
827 proper timing of development and brain growth. *Cell reports* **24**, 3156-3166. e3154 (2018).
828 42 Britton, J. S. & Edgar, B. A. Environmental control of the cell cycle in Drosophila: nutrition
829 activates mitotic and endoreplicative cells by distinct mechanisms. *Development* **125**, 2149-2158
830 (1998).
831 43 Grant, C. E., Bailey, T. L. & Noble, W. S. FIMO: scanning for occurrences of a given motif.
832 *Bioinformatics* **27**, 1017-1018 (2011).
833 44 Kaye, E. G. *et al.* Differential occupancy of two GA-binding proteins promotes targeting of the
834 drosophila dosage compensation complex to the male X chromosome. *Cell reports* **22**, 3227-3239
835 (2018).
836 45 Ribeiro, A. L. *et al.* Naa50/San-dependent N-terminal acetylation of Scc1 is potentially important
837 for sister chromatid cohesion. *Scientific reports* **6**, 1-16 (2016).
838 46 Larochelle, S., Pandur, J., Fisher, R. P., Salz, H. K. & Suter, B. Cdk7 is essential for mitosis and
839 for in vivo Cdk-activating kinase activity. *Genes & development* **12**, 370-381 (1998).
840 47 Lee, C.-Y. *et al.* Drosophila Aurora-A kinase inhibits neuroblast self-renewal by regulating
841 aPKC/Numb cortical polarity and spindle orientation. *Genes & development* **20**, 3464-3474 (2006).
842 48 Curt, J. R., Salmani, B. Y. & Thor, S. Anterior CNS expansion driven by brain transcription factors.
843 *Elife* **8**, e45274 (2019).
844 49 Song, H.-J. *et al.* The fruitless gene is required for the proper formation of axonal tracts in the
845 embryonic central nervous system of Drosophila. *Genetics* **162**, 1703-1724 (2002).
846 50 Zaharieva, E., Haussmann, I. U., Brauer, U. & Soller, M. Concentration and Localization of
847 Coexpressed ELAV/Hu Proteins Control Specificity of mRNA Processing. *Mol Cell Biol* **35**, 3104-
848 3115, doi:10.1128/MCB.00473-15 (2015).
849 51 Turki-Judeh, W. & Courey, A. J. in *Current topics in developmental biology* Vol. 98 65-96
850 (Elsevier, 2012).

851 52 Neumüller, Ralph A. *et al.* Genome-Wide Analysis of Self-Renewal in Drosophila Neural Stem
852 Cells by Transgenic RNAi. *Cell Stem Cell* **8**, 580-593,
853 doi:https://doi.org/10.1016/j.stem.2011.02.022 (2011).
854 53 Weake, V. M. *et al.* SAGA-mediated H2B deubiquitination controls the development of neuronal
855 connectivity in the Drosophila visual system. *The EMBO journal* **27**, 394-405 (2008).
856 54 Janssens, D. H. *et al.* Earmuff restricts progenitor cell potential by attenuating the competence to
857 respond to self-renewal factors. *Development* **141**, 1036-1046 (2014).
858 55 Southall, T. D., Davidson, C. M., Miller, C., Carr, A. & Brand, A. H. Dedifferentiation of neurons
859 precedes tumor formation in Lola mutants. *Dev Cell* **28**, 685-696 (2014).
860 56 Arefin, B., Parvin, F., Bahrampour, S., Stadler, C. B. & Thor, S. Drosophila Neuroblast Selection
861 Is Gated by Notch, Snail, SoxB, and EMT Gene Interplay. *Cell reports* **29**, 3636-3651. e3633
862 (2019).
863 57 Contreras, E. G., Egger, B., Gold, K. S. & Brand, A. H. Dynamic Notch signalling regulates neural
864 stem cell state progression in the Drosophila optic lobe. *Neural development* **13**, 1-11 (2018).
865 58 Hakes, A. E. & Brand, A. H. Neural stem cell dynamics: the development of brain tumours. *Current*
866 *Opinion in Cell Biology* **60**, 131-138 (2019).
867 59 Egger, B., Gold, K. S. & Brand, A. H. Notch regulates the switch from symmetric to asymmetric
868 neural stem cell division in the Drosophila optic lobe. *Development* **137**, 2981-2987 (2010).
869 60 Chell, J. M. & Brand, A. H. Nutrition-responsive glia control exit of neural stem cells from
870 quiescence. *Cell* **143**, 1161-1173 (2010).
871 61 Lanet, E., Gould, A. P. & Maurange, C. Protection of neuronal diversity at the expense of neuronal
872 numbers during nutrient restriction in the Drosophila visual system. *Cell reports* **3**, 587-594 (2013).
873 62 Choksi, S. P. *et al.* Prospero acts as a binary switch between self-renewal and differentiation in
874 Drosophila neural stem cells. *Dev Cell* **11**, 775-789 (2006).
875 63 Knoblich, J. A. & Jan, Y. N. Asymmetric segregation of Numb and Prospero during cell division.
876 *Nature* **377**, 624-627 (1995).

877 64 Colonques, J., Ceron, J., Reichert, H. & Tejedor, F. J. A transient expression of Prospero promotes
878 cell cycle exit of Drosophila postembryonic neurons through the regulation of Dacapo. *PLoS One*
879 **6**, e19342 (2011).
880 65 Robinow, S. & White, K. The locus elav of Drosophila melanogaster is expressed in neurons at all
881 developmental stages. *Developmental biology* **126**, 294-303 (1988).
882 66 Pereanu, W., Shy, D. & Hartenstein, V. Morphogenesis and proliferation of the larval brain glia in
883 Drosophila. *Developmental biology* **283**, 191-203 (2005).
884 67 Kanai, M. I. *et al.* Regulation of neuroblast proliferation by surface glia in the Drosophila larval
885 brain. *Scientific Reports* **8**, 3730, doi:10.1038/s41598-018-22028-y (2018).
886 68 Xiong, W.-C., Okano, H., Patel, N. H., Blendy, J. A. & Montell, C. repo encodes a glial-specific
887 homeo domain protein required in the Drosophila nervous system. *Genes & development* **8**, 981-
888 994 (1994).
889 69 Lin, D. M. & Goodman, C. S. Ectopic and increased expression of Fasciclin II alters motoneuron
890 growth cone guidance. *Neuron* **13**, 507-523 (1994).
891 70 Johnson, M. R., Stephenson, R. A., Ghaemmaghami, S. & Welte, M. A. Developmentally regulated
892 H2Av buffering via dynamic sequestration to lipid droplets in Drosophila embryos. *Elife* **7**, e36021
893 (2018).
894 71 McHugh, B. *et al.* Invadolysin: a novel, conserved metalloprotease links mitotic structural
895 rearrangements with cell migration. *The Journal of cell biology* **167**, 673-686 (2004).
896 72 Rao, S. G. *et al.* Invadolysin acts genetically via the SAGA complex to modulate chromosome
897 structure. *Nucleic acids research* **43**, 3546-3562 (2015).
898 73 Cobbe, N. *et al.* The conserved metalloprotease invadolysin localizes to the surface of lipid
899 droplets. *Journal of cell science* **122**, 3414-3423 (2009).
900 74 Kramer, J. M., Davidge, J. T., Lockyer, J. M. & Staveley, B. E. Expressionof Drosophila FOXO
901 regulates growth and can phenocopy starvation. *BMC developmental biology* **3**, 5 (2003).
902 75 Huang, H. & Tindall, D. J. Dynamic FoxO transcription factors. *J Cell Sci* **120**, 2479-2487 (2007).

903 76 Wei, J.-Y., Chung, P.-C., Chu, S.-Y. & Yu, H. H. FOXO regulates cell fate specification of
904 Drosophila ventral olfactory projection neurons. *Journal of neurogenetics* **33**, 33-40 (2019).
905 77 Sano, H. Coupling of growth to nutritional status: The role of novel periphery-to-brain signaling
906 by the CCHa2 peptide in Drosophila melanogaster. *Fly* **9**, 183-187 (2015).
907 78 Okamoto, N. & Nishimura, T. Signaling from Glia and Cholinergic Neurons Controls Nutrient-
908 Dependent Production of an Insulin-like Peptide for Drosophila Body Growth. *Dev Cell* **35**, 295-
909 310, doi:10.1016/j.devcel.2015.10.003 (2015).
910 79 Chotard, C., Leung, W. & Salecker, I. glial cells missing and gcm2 cell autonomously regulate both
911 glial and neuronal development in the visual system of Drosophila. *Neuron* **48**, 237-251 (2005).
912 80 Chen, Z. *et al.* A unique class of neural progenitors in the Drosophila optic lobe generates both
913 migrating neurons and glia. *Cell reports* **15**, 774-786 (2016).
914 81 Ile, K. E., Tripathy, R., Goldfinger, V. & Renault, A. D. Wunen, a Drosophila lipid phosphate
915 phosphatase, is required for septate junction-mediated barrier function. *Development* **139**, 2535-
916 2546 (2012).
917 82 DeSalvo, M. K. *et al.* The Drosophila surface glia transcriptome: evolutionary conserved blood-
918 brain barrier processes. *Frontiers in neuroscience* **8**, 346 (2014).
919 83 Loyer, N. & Januschke, J. The last-born daughter cell contributes to division orientation of
920 Drosophila larval neuroblasts. *Nature Communications* **9**, 3745, doi:10.1038/s41467-018-06276-0
921 (2018).
922 84 Yang, P.-L., Hsu, T.-H., Wang, C.-W. & Chen, R.-H. Lipid droplets maintain lipid homeostasis
923 during anaphase for efficient cell separation in budding yeast. *Molecular biology of the cell* **27**,
924 2368-2380 (2016).
925 85 Cruz, A. L. *et al.* Cell cycle progression regulates biogenesis and cellular localization of lipid
926 droplets. *Molecular and cellular biology* **39** (2019).

927 86 Bernardoni, R., Kammerer, M., Vonesch, J.-L. & Giangrande, A. Gliogenesis depends on
928 glide/gcm through asymmetric division of neuroglioblasts. *Developmental biology* **216**, 265-275
929 (1999).
930 87 Bossing, T., Udolph, G., Doe, C. Q. & Technau, G. M. The Embryonic Central Nervous System
931 Lineages ofDrosophila melanogaster: I. Neuroblast Lineages Derived from the Ventral Half of the
932 Neuroectoderm. *Developmental biology* **179**, 41-64 (1996).
933 88 Schmid, A., Chiba, A. & Doe, C. Q. Clonal analysis of Drosophila embryonic neuroblasts: neural
934 cell types, axon projections and muscle targets. *Development* **126**, 4653-4689 (1999).
935 89 Udolph, G., Rath, P. & Chia, W. A requirement for Notch in the genesis of a subset of glial cells
936 in the Drosophila embryonic central nervous system which arise through asymmetric divisions.
937 *Development* **128**, 1457-1466 (2001).
938 90 Tastan, Ö. Y. & Liu, J.-L. CTP synthase is required for optic lobe homeostasis in Drosophila.
939 *Journal of genetics and genomics* **42**, 261-274 (2015).
940 91 Maroni, G. & Stamey, S. Use of blue food to select synchronous, late third instar larvae. *Dros. Inf.*
941 *Serv* **59**, 142-143 (1983).
942 92 Andrews, S. (Babraham Bioinformatics, Babraham Institute, Cambridge, United Kingdom,
943 2010).
944 93 Kim, D., Langmead, B. & Salzberg, S. hisat2. *Nature methods* (2015).
945 94 Anders, S., Pyl, P. T. & Huber, W. HTSeq—a Python framework to work with high-throughput
946 sequencing data. *Bioinformatics* **31**, 166-169 (2015).
947 95 Love, M., Anders, S. & Huber, W. Differential analysis of count data–the DESeq2 package.
948 *Genome Biol* **15**, 10.1186 (2014).
949 96 Raudvere, U. *et al.* g:Profiler: a web server for functional enrichment analysis and conversions of
950 gene lists (2019 update). *Nucleic Acids Research* **47**, W191-W198, doi:10.1093/nar/gkz369 (2019).
951 97 Conard, A. M. *et al.* TIMEOR: a web-based tool to uncover temporal regulatory mechanisms from
952 multi-omics data. *bioRxiv* (2020).

953 98 Yu, G., Wang, L.-G., Han, Y. & He, Q.-Y. clusterProfiler: an R package for comparing biological
954 themes among gene clusters. *Omics: a journal of integrative biology* **16**, 284-287 (2012).
955 99 Turner, F. R. & Mahowald, A. P. Scanning electron microscopy of Drosophila melanogaster
956 embryogenesis: II. Gastrulation and segmentation. *Developmental biology* **57**, 403-416 (1977).
957

958 **Acknowledgements**

959 We thank Dr. Edward A. Kravitz for providing MAT laboratory space and contributing to supply costs for
960 completion of this study, Dr. Yick-Bun Chan for experimental support and assistance with DEG analysis
961 and Dr. Yiannis Savva for experimental support. We would also like to thank Dr. Séverine Trannoy for
962 critical reading of this manuscript. We thank the Harvard Medical School Neurobiology Department and
963 the Neurobiology Imaging Facility for consultation and instrument availability that supported this work.
964 This facility is supported in part by the Neural Imaging Center as part of an NINDS P30 Core Center grant
965 #NS072030. This work was supported in part by a Harvard Medical School Fix Fund Postdoctoral
966 Fellowship to M.A.T and by US National Institute of Health grants to E.N.L and E.A.K (R35 GM126994-
967 01 and R35 GM118137).
968

969 **Contributions**

970 MAT and E.N.L conceived the study and M.A.T designed the study. M.A.T performed
971 immunohistochemistry and imaging, collection of RNA-seq samples and analysis of RNA-seq DEG results.
972 L.X contributed to sample collection for RNA-seq experiments and immunohistochemistry, E.N
973 contributed in size experiments and A.M.C contributed in RNA-seq data analysis. M.A.T prepared figures
974 and wrote the original draft while M.A.T and E.N.L curated the manuscript with input from all authors.
975

976 **Declaration of Interests**

977 The authors declare no competing interests.
978

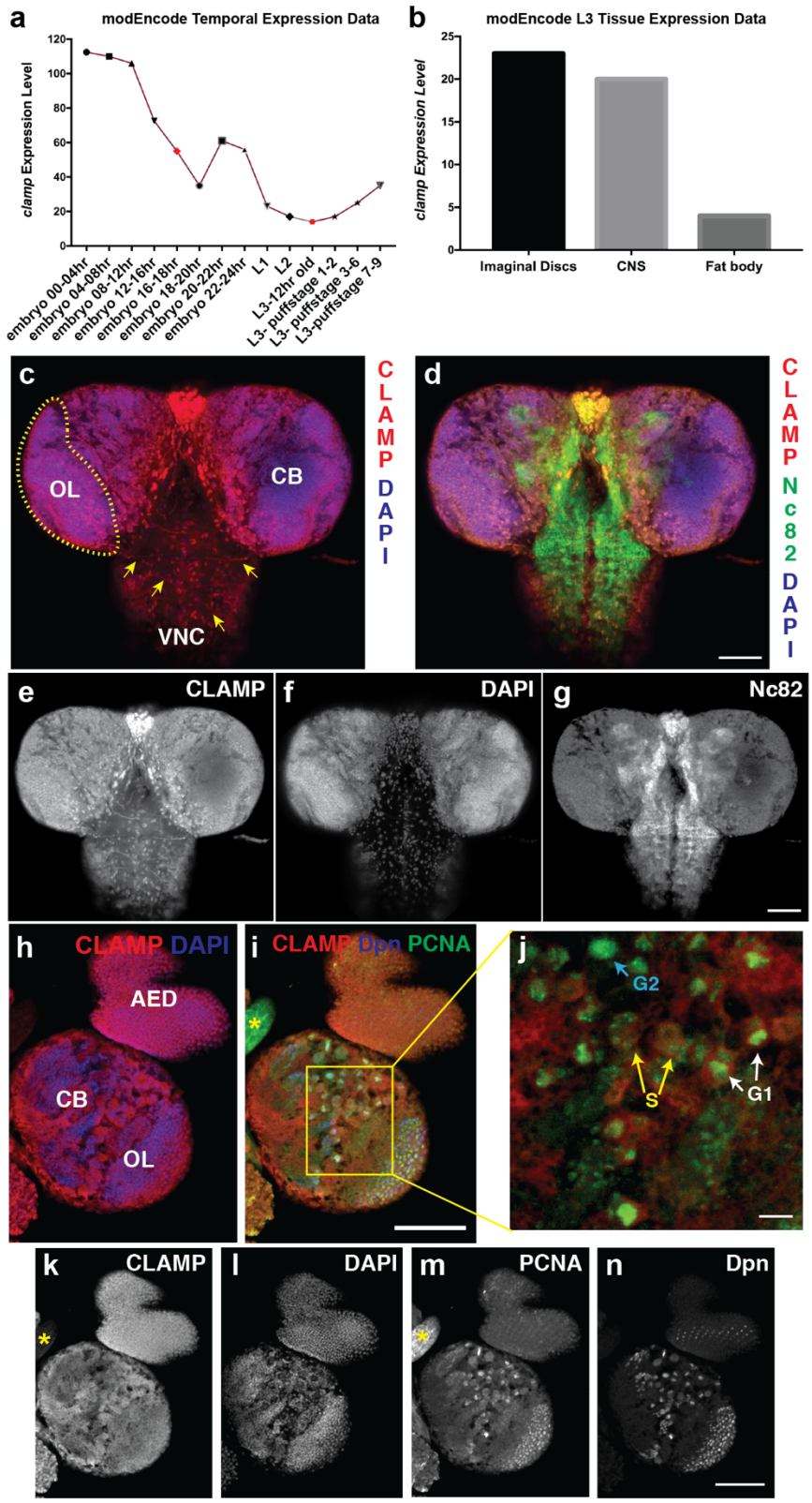
a
modEncode Temporal Expression Data
clamp Expression Level
120
100
80
60
40
20
0
embryo 00-04hr
embryo 04-08hr
embryo 08-12hr
embryo 12-16hr
embryo 16-18hr
embryo 18-20hr
embryo 20-22hr
embryo 22-24hr
L1
L2
L3-12hr old
L3- puffstage 1-2
L3- puffstage 3-6
L3-puffstage 7-9
b
modEncode L3 Tissue Expression Data
clamp Expression Level
25
20
15
10
5
0
Imaginal Discs
CNS
Fat body
c
OL
CB
VNC
CLAMP DAPI
d
CLAMP Nc82 DAPI
e
CLAMP
f
DAPI
g
Nc82
h
CLAMP DAPI
AED
CB
OL
i
CLAMP Dpn PCNA
*
j
G2
S
G1
k
CLAMP
*
l
DAPI
m
PCNA
*
n
Dpn

979

980 **Figure 1 CLAMP is ubiquitously expressed throughout the L3 nervous system and is present in**
981 **proliferating neuroblasts.** (a) Temporal expression data from modEncode (Flybase) reveal that *clamp*
982 expression levels decrease as embryonic development proceeds and as the maternal transcripts are used-up
983 and reach a nadir at 18-20 hours after egg lay, which is then followed by a sharp increase just before
984 embryonic development is completed. During the larval stages *clamp* expression decreases until L3, where
985 it slowly starts to increase again before the pupa stage. (b) Tissue specific L3 expression data, reveal that
986 *clamp* is most highly expressed in the developing imaginal disks, the CNS and also the fat body.
987 (c-g) CLAMP is expressed both in the L3 central nervous system, specifically in the optic lobe (OL, yellow
988 dashed outline), central brain, (CB) and in the ventral nerve cord (VNC). (c, d) CLAMP is present in the
989 nucleus throughout the nervous system as seen by co-staining with DAPI and Nc82, which marks the
990 synaptic processes. In the VNC it is also observed in the neuronal processes (c, arrows). Panels e-g show
991 individual staining channels. (h-n) Higher resolution images reveal high expression of CLAMP in the
992 developing CB and OL and specifically in proliferating NSCs marked by Deadpan (Dpn) and Proliferating
993 cell nuclear antigen (PCNA). (j) Magnification of the boxed area in panel i, reveals that CLAMP is present
994 in cycling NSCs during different cell cycle phases according to the PCNA nuclear distribution. Star (*) in
995 panels k and m indicates an artifact. Scale bars: 50 µm and 25 µm in j.
996
997
998
999

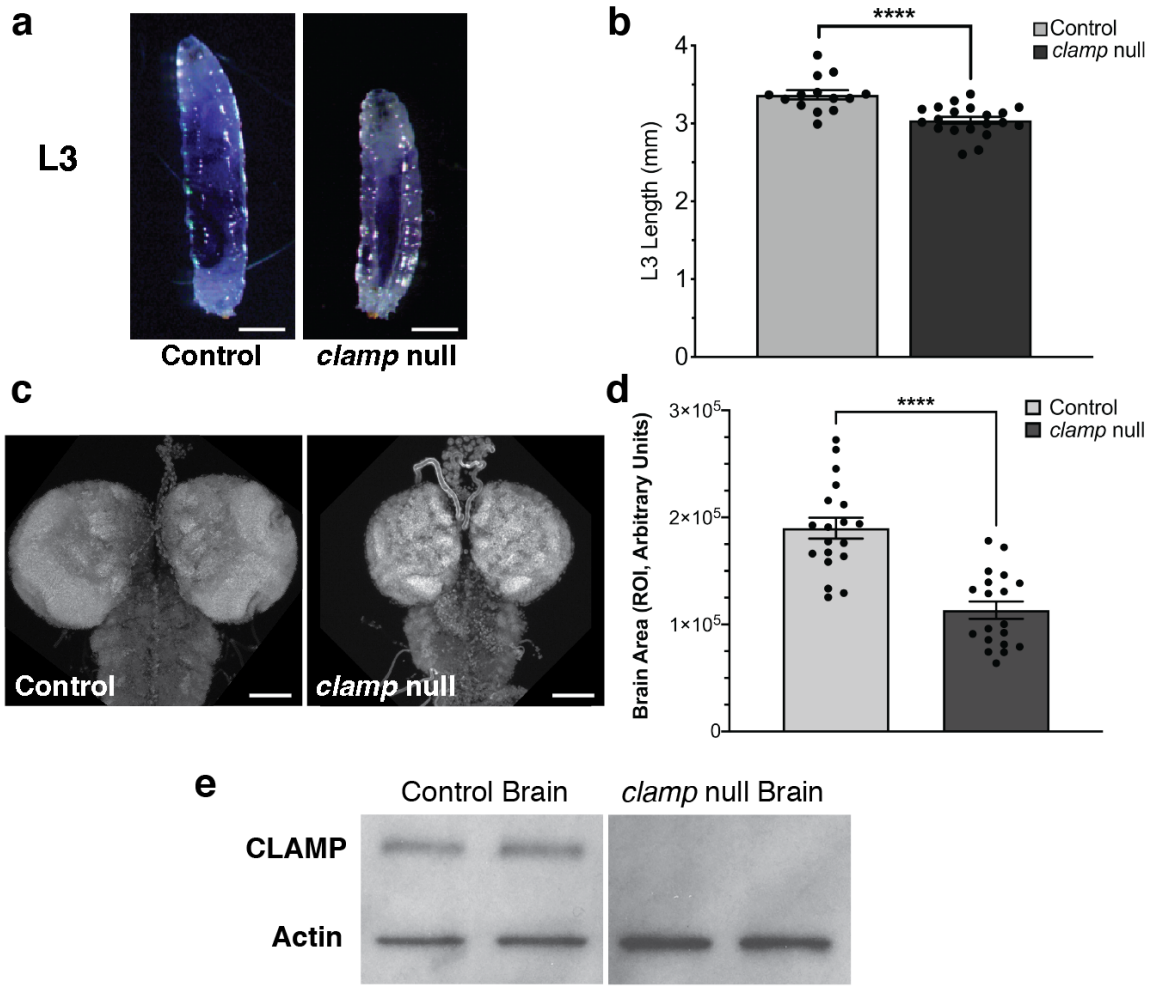

1000

1001

1002 **Figure 2 Lack of CLAMP results in growth deficits both in the body and the nervous system** (a, b)
1003 Mutant *clamp* null L3 larvae are considerably smaller in size, compared to control L3s (Mean length ±
1004 SEM; Control: 3.369 ± 0.06031, n=14; *clamp* null: 3.041 ± 0.04371, n=20; ttest p< 0.0001). (c, d) This
1005 reduction is maintained at the CNS level of *clamp* null L3 larvae (Mean normalized brain area ± SEM;
1006 Control: 1.001 ± 0.0485, n=20; *clamp* null: 0.601 ± 0.04052, n=20; ttest p< 0.0001). (e) Western blot for
1007 CLAMP in samples from L3 brain lysates from control and *clamp* null L3 showing the absence of CLAMP
1008 protein (n=2 per condition). Scale bars: 1 mm in a; 50 μm in c.

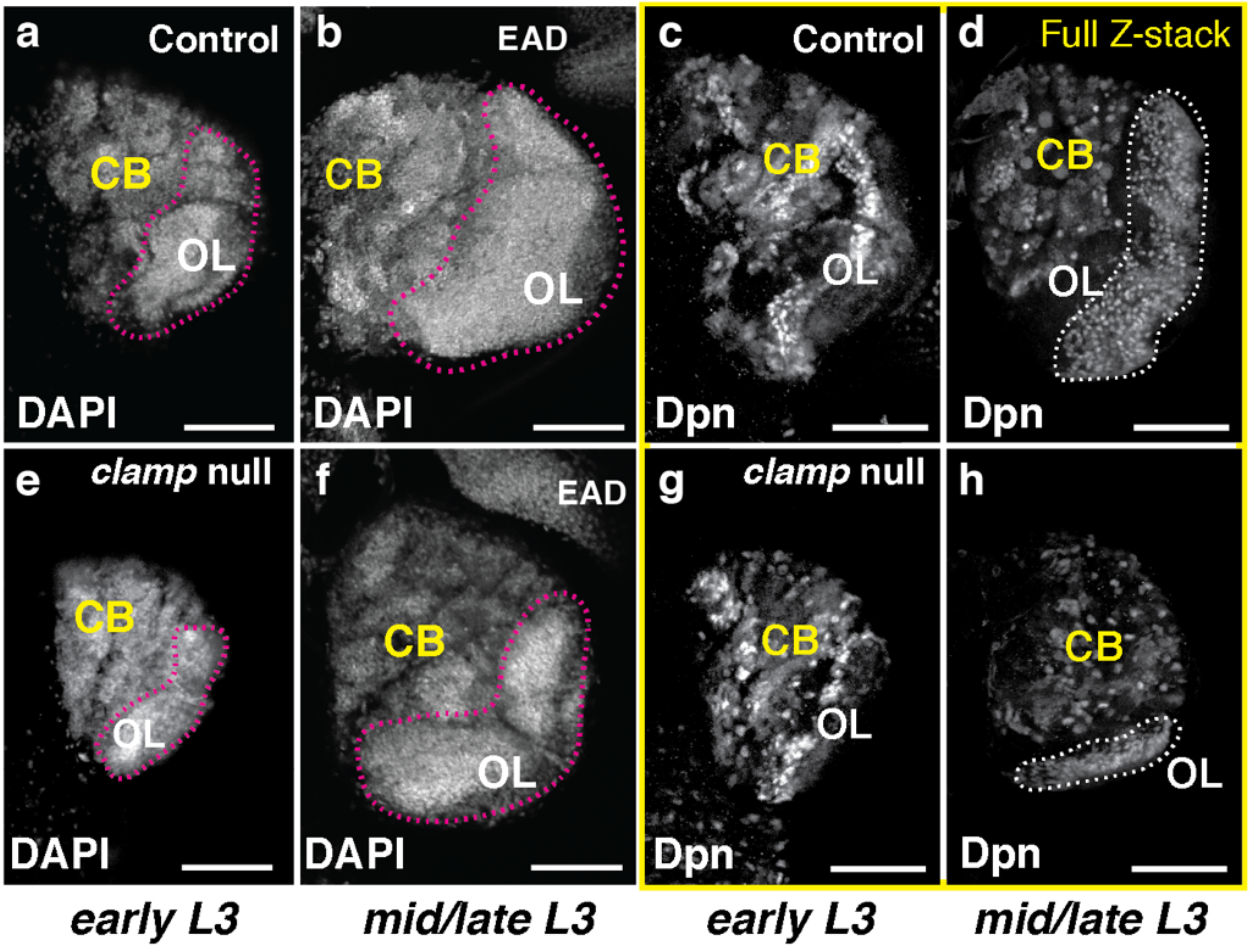

1009

1010 **Figure 3 Lack of CLAMP greatly affects brain development and causes defects in optic lobe**
1011 **formation.** (a, b and e, f) Brain development in the *clamp* null L3 is severely impaired from the early L3
1012 stage, while even at the mid/late L3 stage, *clamp* null brains resemble early L3 control brains. (c, d and g,h)
1013 Full z-stacks of L3 brains showing the distribution of Deadpan (Dpn) -positive NSCs areas, reveals that
1014 NSCs development both in the central brain (CB) and the optic lobe (OL) of the null are impaired, starting
1015 from the early L3 stage and continuing to the mid/late L3 stage. Especially impaired is the OL development
1016 as seen by the reduction in the Dpn+ area indicated with the white dashed outlined areas. EAD: eye antenna
1017 disk. Panels a, b, e and f are 3 optical sections whereas c, d, g and h are full z-stacks throughout the brain.
1018 Scale bars: 50 μm.

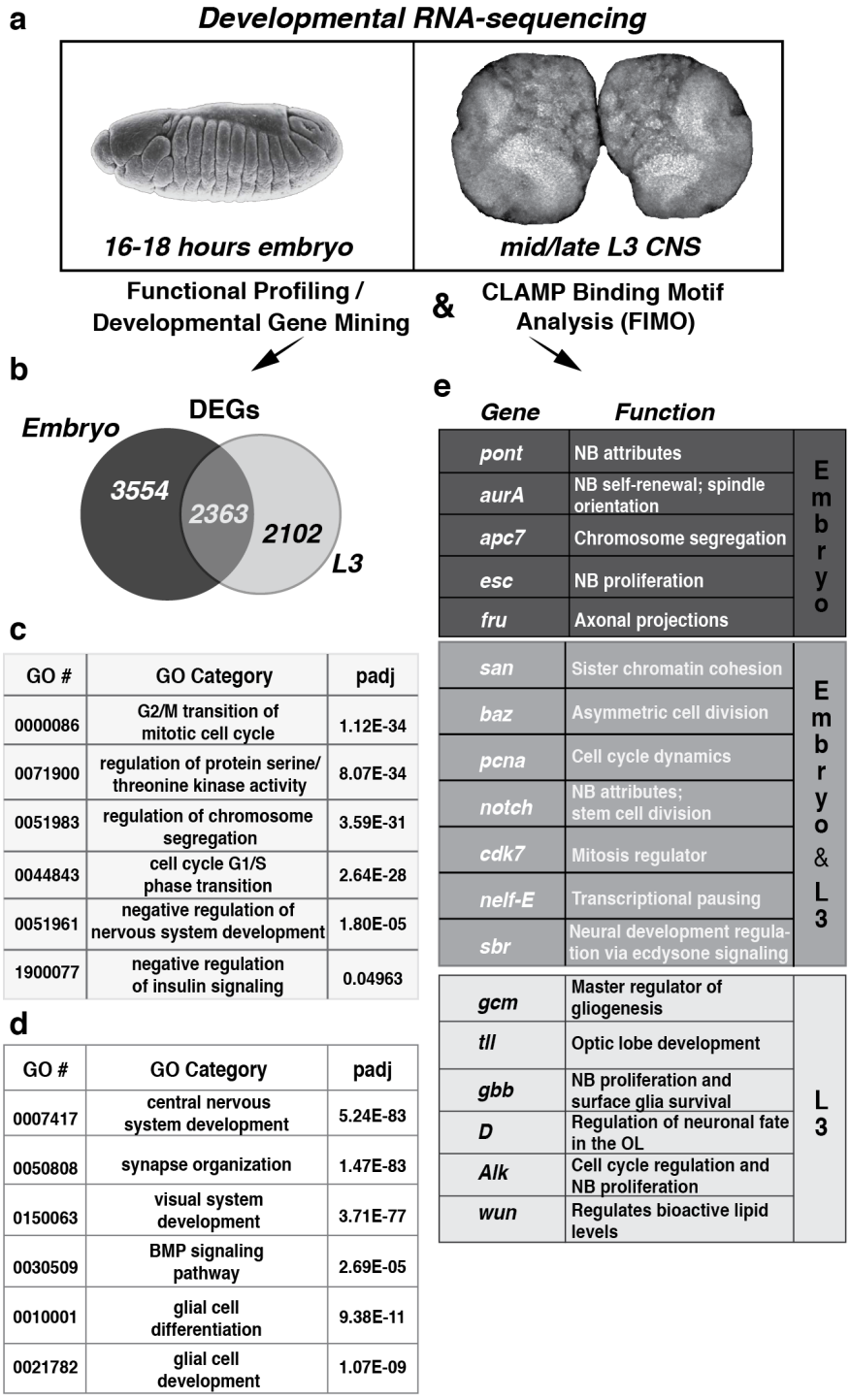

GO #	GO Category	padj
0000086	G2/M transition of mitotic cell cycle	1.12E-34
0071900	regulation of protein serine/ threonine kinase activity	8.07E-34
0051983	regulation of chromosome segregation	3.59E-31
0044843	cell cycle G1/S phase transition	2.64E-28
0051961	negative regulation of nervous system development	1.80E-05
1900077	negative regulation of insulin signaling	0.04963

GO #	GO Category	padj
0007417	central nervous system development	5.24E-83
0050808	synapse organization	1.47E-83
0150063	visual system development	3.71E-77
0030509	BMP signaling pathway	2.69E-05
0010001	glial cell differentiation	9.38E-11
0021782	glial cell development	1.07E-09

1019

1020 **Figure 4 CLAMP is implicated in transcriptomic networks that regulate the proliferation and**
1021 **differentiation of NSCs.** (a) Experimental workflow for RNA sequencing data generation and DEG meta-
1022 analysis. Embryo panel is scanning electron image of a late stage embryo from[99]. (b) Venn diagram of
1023 DEGs in the *clamp* null embryo and L3. (c, d) GO analysis of the *clamp* null DEGs revealed high

1024 enrichment in categories related to cell cycle dynamics and neural development. (e) Find Individual Motif
1025 Occurrences (FIMO) analysis of the DEGs for the CLAMP binding motif, revealed that critical regulators
1026 of neural development and mitosis are putative targets for CLAMP binding both at the embryonic and L3
1027 stage.
1028
1029
1030
1031
1032
1033
1034
1035
1036
1037
1038
1039
1040
1041

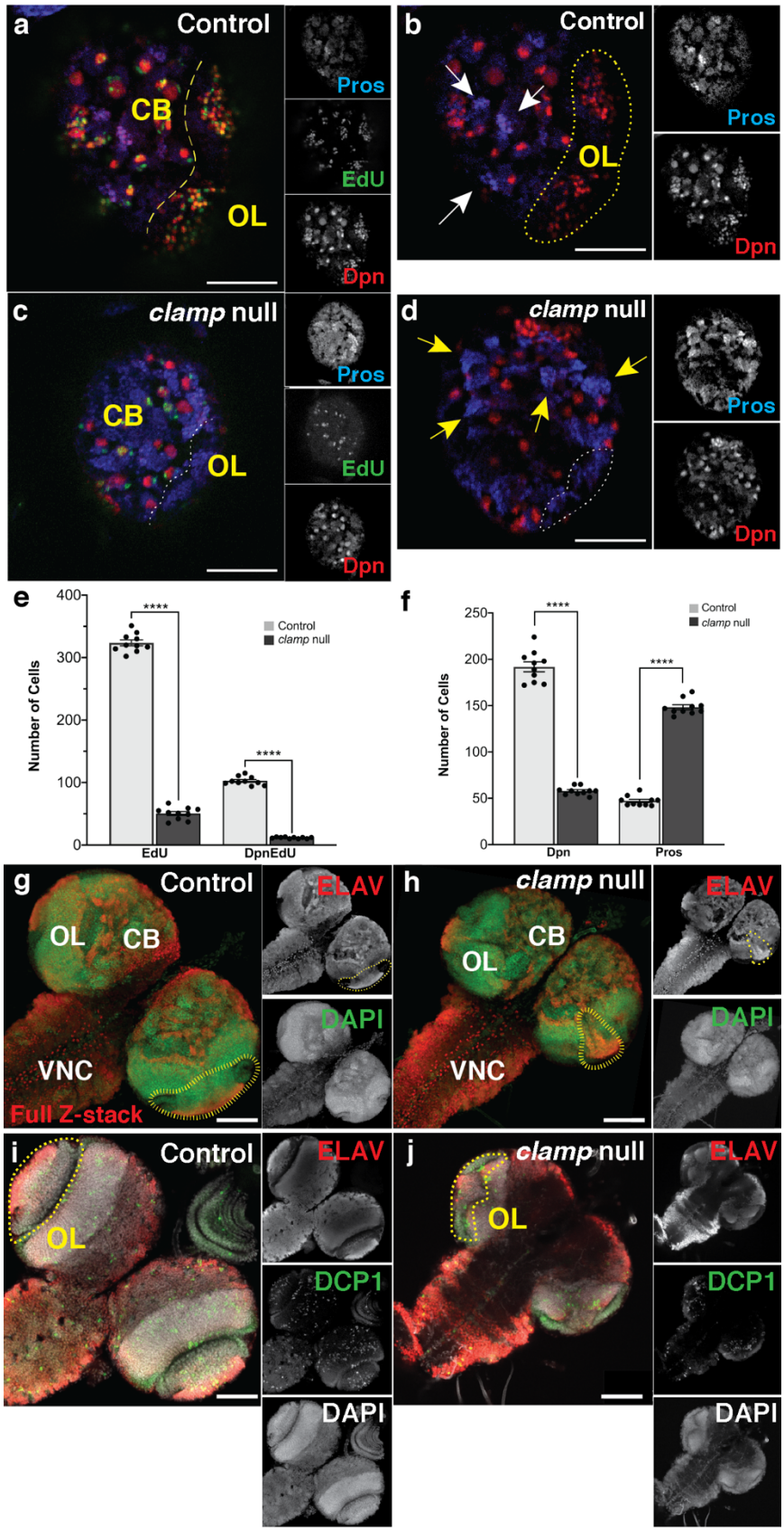
a
Control
CB
OL
Pros
EdU
Dpn
b
Control
OL
Pros
Dpn
c
clamp null
CB
OL
Pros
EdU
Dpn
d
clamp null
Pros
Dpn
e
Number of Cells
400
300
200
100
0
****
****
Control
clamp null
EdU
DpnEdU
f
Number of Cells
250
200
150
100
50
0
****
****
Control
clamp null
Dpn
Pros
g
Control
OL
CB
VNC
Full Z-stack
ELAV
DAPI
h
clamp null
CB
OL
VNC
ELAV
DAPI
i
Control
OL
ELAV
DCP1
DAPI
j
clamp null
OL
ELAV
DCP1
DAPI

1042

1043 **Figure 5 Lack of CLAMP impairs neural stem cell proliferation and promotes precocious**
1044 **differentiation**. (a-d) Proliferation of NSCs as seen by EdU labeling, is highly reduced in the *clamp* null
1045 brain, with the most evident impact being on OL NSCs (panels a and c, dashed lines indicate the OL). In
1046 parallel, nuclear Pros+ clusters indicate acquisition of neuronal fate, are more evident in the *clamp* null
1047 brains (panels b and d, arrows). (e) Both the total number of proliferating stem cells (EdU^+ Mean ± SEM,
1048 Control: 323.6 ± 4.679; *clamp* null: 50.40 ± 3.174; $p<0.0001$; n=10) and of proliferating Dpn^+ NSCs is
1049 reduced (Dpn^+EdU^+ Mean ± SEM; Control 102.6 ± 2.141; *clamp* null 11.50 ± 0.3727; n=10). (f) The
1050 reduction in total Dpn+ cells (Dpn^+ Mean ± SEM, Control: 191.9 ± 5.313; *clamp* null: 57.90 ± 1.402; p
1051 <0.0001; n = 10), is accompanied by a respective increase in Pros+ cells in the *clamp* null brains ($Pros^+$
1052 Mean ± SEM, Control: 47.1 ± 1.716; *clamp* null: 148.3 ± 2.629; $p <0.0001$; n = 10). (g, h) Additionally,
1053 despite having an increase in the neuronal marker Elav in the *clamp* null brains, the OL development is
1054 impaired compared to controls (outlines). (i, j) Apoptotic cells marked with DCP1 are more in the OL of
1055 the null compared to a more ubiquitous distribution in the control. CB, central brain; OL, optic lobe; VNC:
1056 ventral nerve cord. Scale bars: a-d, 100 µm; g and h, 50 µm.
1057
1058
1059
1060
1061
1062
1063
1064
1065
1066
1067
1068

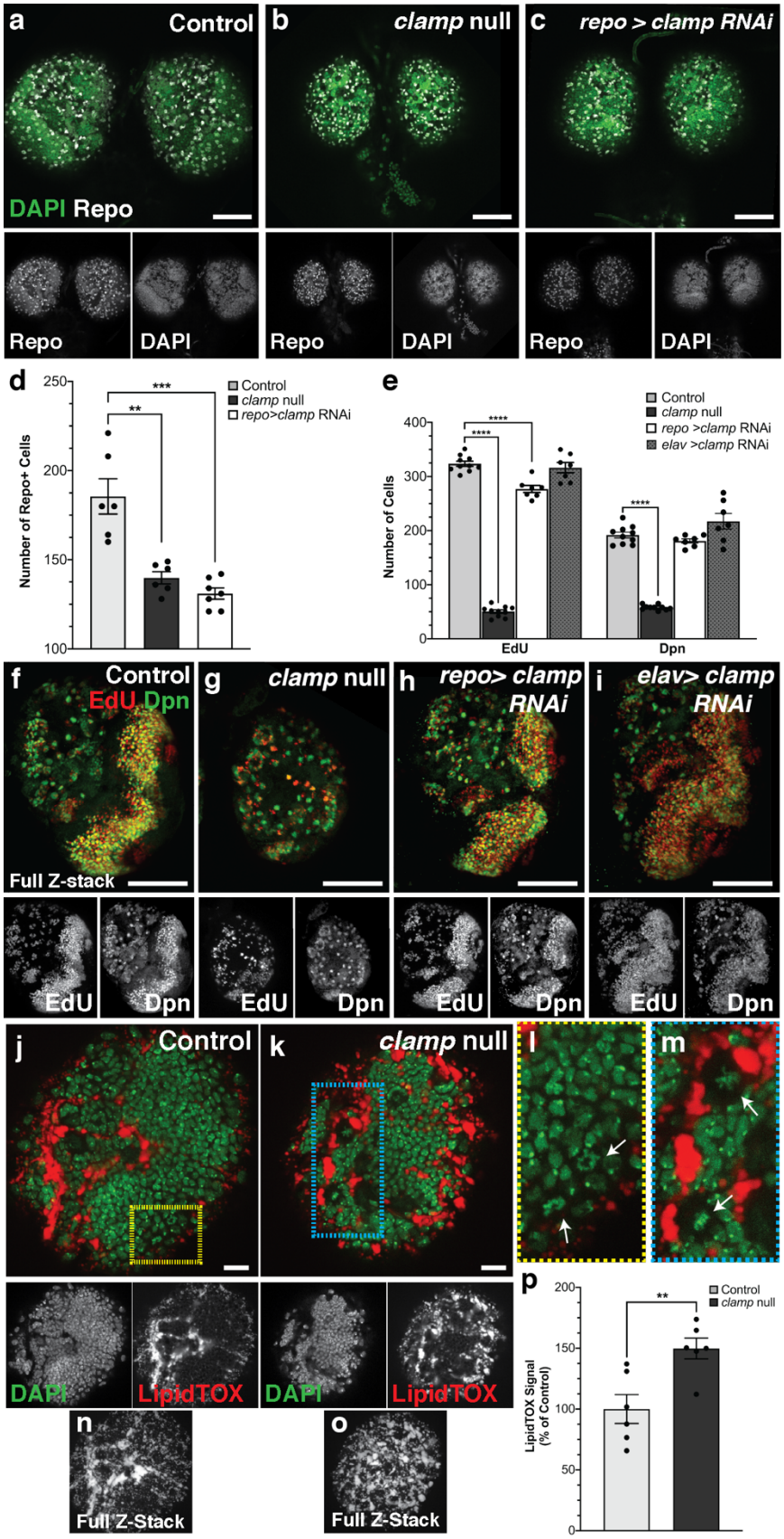
a
Control
DAPI Repo
Repo
DAPI
b
clamp null
Repo
DAPI
c
repo > clamp RNAi
Repo
DAPI
d
Number of Repo+ Cells
250
200
150
100
***
**
Control
clamp null
repo>clamp RNAi
e
Number of Cells
400
300
200
100
0
****
****
****
Control
clamp null
repo >clamp RNAi
elav >clamp RNAi
EdU
Dpn
f
Control
EdU Dpn
Full Z-stack
EdU
Dpn
g
clamp null
EdU
Dpn
h
repo> clamp RNAi
EdU
Dpn
i
elav> clamp RNAi
EdU
Dpn
j
Control
DAPI
LipidTOX
k
clamp null
DAPI
LipidTOX
l
m
n
Full Z-Stack
o
Full Z-Stack
p
LipidTOX Signal (% of Control)
200
150
100
50
0
**
Control
clamp null

1069

1070 **Figure 6 Glial-CLAMP surface glia generation and NSC proliferation** (a-e) Surface glia (SG) is
1071 reduced by ~25% in the *clamp* null brain compared to controls (% SG Repo$^+$ ± SEM, *Control*: 99.98 ±
1072 5.328; *clamp* null: 75.37 ± 1.843; n=6) whereas, (e-i) proliferating NSCs (EdU$^+$ ± SEM, *Control:* 323.6 ±
1073 *4.679; clamp* null: 50.40 ± *3.174*) and NSCs (Dpn$^+$ ± SEM, *Control:* 191.9 ± *5.313; clamp* null: 57.90 ±
1074 *1.402*) are also reduced in numbers. Glial-specific *clamp* knock-down (*repo>clamp RNAi*) promotes a
1075 similar reduction in SG numbers ((% SG Repo$^+$ ± SEM, *repo>clamp RNAi* 131.0 ± 3.162) and promotes a
1076 reduction in proliferating NSCs (*repo>clamp RNAi* EdU$^+$ ± SEM*:* 277 ± 6.572; Dpn$^+$ ± SEM: 181 ± 3.964),
1077 but to a lesser extend as the one seen in the *clamp* null. Neuronal-specific clamp KD (*elav>clamp RNAi*)
1078 does not affect NSC proliferation and numbers NSCs (*elav>clamp RNAi* EdU$^+$ ± SEM*:* 316. ± 9.519; Dpn$^+$
1079 ± SEM: 217 ± 14.45),. (j-p) Staining with the neutral lipid-specific dye LipidTOX, revealed an altered
1080 distribution of LDs in the *clamp* null brain compared to controls and (p) a ~50% increase in LDs in the
1081 *clamp* null brain, compared to controls (% LipidTOX signal ± SEM; Control: 100 ± 11.86; *clamp* null:
1082 149.8 ± 8.599, n=6). (n-o) This increase is also evident in the panels showing a full z-stack for each
1083 condition. Panels l and m, represent magnification of the boxed areas in panels j and k respectively, where,
1084 large LD formations are observed surrounding dividing NSCs in the *clamp* null. Scale bars 100 µm.
1085
1086
1087
1088
1089
1090
1091
1092
1093
1094
1095

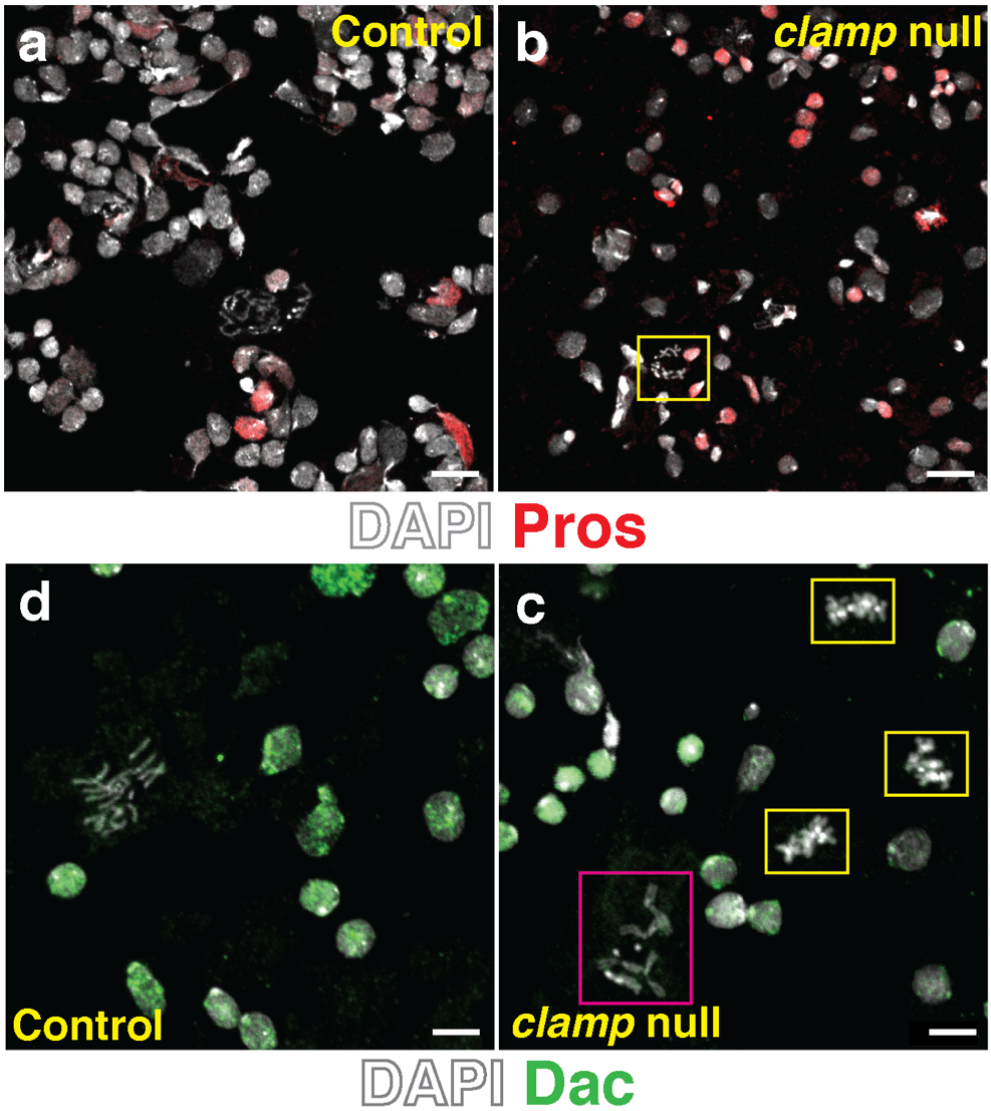

1096

1097 **Figure 7 Lack of CLAMP results in aberrant mitotic chromosome morphology** (a,b) Chromosomal
1098 preparations of mitotic neuroblasts from L3 brains reveal the presence of mitotic chromosomes with altered
1099 morphology in the *clamp* null (rectangle in b). Additionally, in the *clamp* null condition more Pros+ positive
1100 nuclei are present, signaling more neuronal differentiation compared to controls. (d, c) Higher
1101 magnification images showing that mitotic NSC chromosomes in the *clamp* null in their majority are hyper-
1102 condensed and stubby (c, yellow rectangles) while the nuclei appear smaller compared to controls.
1103 Additionally, in the *clamp* null preparations, less nuclei are positive for Dac, a regulator of OL development.
1104 Scale bars, 100 μm.

1105

Gene Name	log2FC	padj
elav	0.44	0.043
ewg	NA	NA
clamp	-1	6.39E-14
CG12299	-0.70	0.0001
gro	-0.88	2.45E-06
CG8924	-1.12	1.15E-10
JIL-1	NA	NA
osk	-4.76	1.67E-11
ac3	0.54	4.87E-05
cdc16	-0.83	0.005
Ibf1	-0.78	0.0002
Bcl7-like	-0.93	2.92E-11

Table 1: Functional interactors of clamp as identified by Haussman et al., 2008

Gene ID	***Gene Name***	***Log2FC***	***padj***	***Function***
FBgn0044047	*Dilp6*	-3.028	4.38E-42	OL development/Glia Neuroblast interactions/Insulin Signaling
FBgn0003720	*tll*	-1.71	1.89E-31	OL development
FBgn0031745	*rau*	-1.373	3.42E-18	Glial cell development/differentiation of neurons and glia in the developing eye.
FBgn0014179	*gcm*	-1.281	5.90E-12	Glial cell development-promotes gliogenesis over neurogenesis
FBgn0010433	*ato*	-1.246	3.88E-15	OL development
FBgn0000529	*bsh*	-1.155	1.85E-24	OL development
FBgn0019809	*gcm2*	-1.154	3.97E-20	Has a redundant role with the product of *gcm* in the differentiation of glial cells and subset of neurons[79].
FBgn0031375	*erm*	-1.116	2.76E-19	Cell fate regulator during neurogenesis.
FBgn0000163	*baz*	-1.105	6.44E-10	Bazooka forms a complex with par-6 and aPKC. Functions in cell polarization and ACD.
FBgn0021776	*mira*	-0.99	3.16E-07	Neuroblast proliferation.
FBgn0000137	*ase*	-0.972	1.54E-05	Type I NB attributes.
FBgn0263512	*Vsx2*	-0.956	9.10E-23	OL development.
FBgn0010382	*CycE*	-0.951	0.00131	Cell cycle dynamics.
FBgn0001983	*wor*	-0.94	3.01E-05	Worniu, neuroblast attributes.
FBgn0000320	*eya*	-0.909	2.05E-08	OL development /insulin producing cells differentiation.
FBgn0000404	*CycA*	-0.855	0.010084	Cell cycle progression including G2.
FBgn0025739	*pon*	-0.847	3.66E-07	Contributes to asymmetric localization of numb and the subsequent suppression of Notch signaling.
FBgn0002973	*numb*	-0.845	1.67E-15	Acts via Notch signaling, asymmetric division control.
FBgn0005655	*PCNA*	-0.824	0.00019	Cell cycle dynamics.
FBgn0011674	*insc*	-0.788	1.44E-06	Spindle orientation; asymmetric divisions.
FBgn0037913	*fabp*	-0.72	1.85E-06	Expressed in lipid droplet-forming glial cells.
FBgn0013469	*klu*	-0.713	0.00013	Klumpfuss (*klu*) is a temporal fate determination.
FBgn0005677	*dac*	-0.707	4.97E-11	OL development.
FBgn0010109	*dpn*	-0.665	0.00245	Neuroblast self-renewal -interacts with *klu* and *erm*.
FBgn0004647	*Notch*	-0.642	0.0018	OL development/Stem cell proliferation.
FBgn0000411	*Dichaete (D)*	-0.634	2.56E-08	Nervous system development and OL development.
FBgn0044324	*Chro*	-0.61	0.00021	Neuroblast proliferation. Functions downstream of InR/PI3K/TOR signaling and regulates expression of quiescence-inducing Pros to permit NSC reactivation.
FBgn0005427	*ewg*	-0.533	1.06E-06	Neurogenesis/Synaptogenesis.
FBgn0040080	*pins*	-0.52	0.008985	Partner of Inscutable; involved in ACD and establishment of cell polarity.

1132 *Table 2: Down-regulated genes in the clamp null L3 brain*

Gene ID	***Gene Name***	***Log2Fc***	***padj***	***Function***
FBgn0000014	abd-A	2.983	0.00019	Controls the end of neuroblast proliferation.
FBgn0025879	Timp	2.299	9.57E-23	Coordinates synaptogenesis
FBgn0001258	Ldh	2.353	2.43E-22	Lipid metabolism.
FBgn0003117	pnr	2.106	0.008812	Activator of *proneural* achaete-scute complex genes.
FBgn0011746	ana	1.831	3.97E-20	Encodes a secreted glycoprotein that is expressed in glia and at lower levels in neuroblasts, suppresses neuroblast proliferation.
FBgn0032006	Pvr	1.742	8.56E-22	Glia development /neuroblast proliferation.
FBgn0016032	lbm	1.576	3.84E-21	facilitates synapse assembly
FBgn0037989	ATP8B	1.664	2.18E-20	Flippase, translocates phospholipids from one side of a membrane to the other forming new membrane structures, especially vesicles.
FBgn0031461	daw	1.502	2.82E-05	Regulates insulin release from IPC neurons.
FBgn0041087	wun2	1.249	3.17E-20	Encodes a lipid phosphate phosphatase; expressed in astrocytes.
FBgn0086677	jeb	1.224	1.37E-06	Functions as signaling ligand for the product of Alk.
FBgn0066101	LpR1	0.899	3.91E-21	Cellular uptake of neutral lipids from the circulating protein encoded by apolpp.
FBgn0000416	Sap-r	0.889	2.23E-29	Lysosomal Lipid homeostasis.
FBgn0000546	EcR	0.847	6.72E-06	Ecdysone Receptor.
FBgn0040505	Alk	0.692	0.00014	Employs Ras/ERK and PI3K signalling pathways, functions in multiple contexts including synaptic signaling.
FBgn0001297	kay	0.699	7.62E-12	Specifically expressed in glia.
FBgn0039332	alrm	0.635	0.00038	Glial related.
FBgn0000370	crc	0.61	3.83E-17	Coactivator of the product EcR, promotes expression the molting peptide hormone encoded by ETH.
FBgn0016078	wun	0.558	2.85E-07	Lipid phosphate phosphatase.
FBgn0013342	nSyb	0.506	3.24E-05	Synaptic signaling.
FBgn0030574	sbm	0.504	0.002373	L-type amino acid transporter expressed in glia; essential for proper timing of development and brain growth [41].

1133 *Table 3: UP-regulated genes in the clamp null L3 brain*

1134

1135

1136

1137

1138

1139

1140

1141